UNIVERSITAT POLITÈCNICA DE VALÈNCIA

Escola Tècnica Superior d'Enginyeria Agronòmica i del Medi Natural

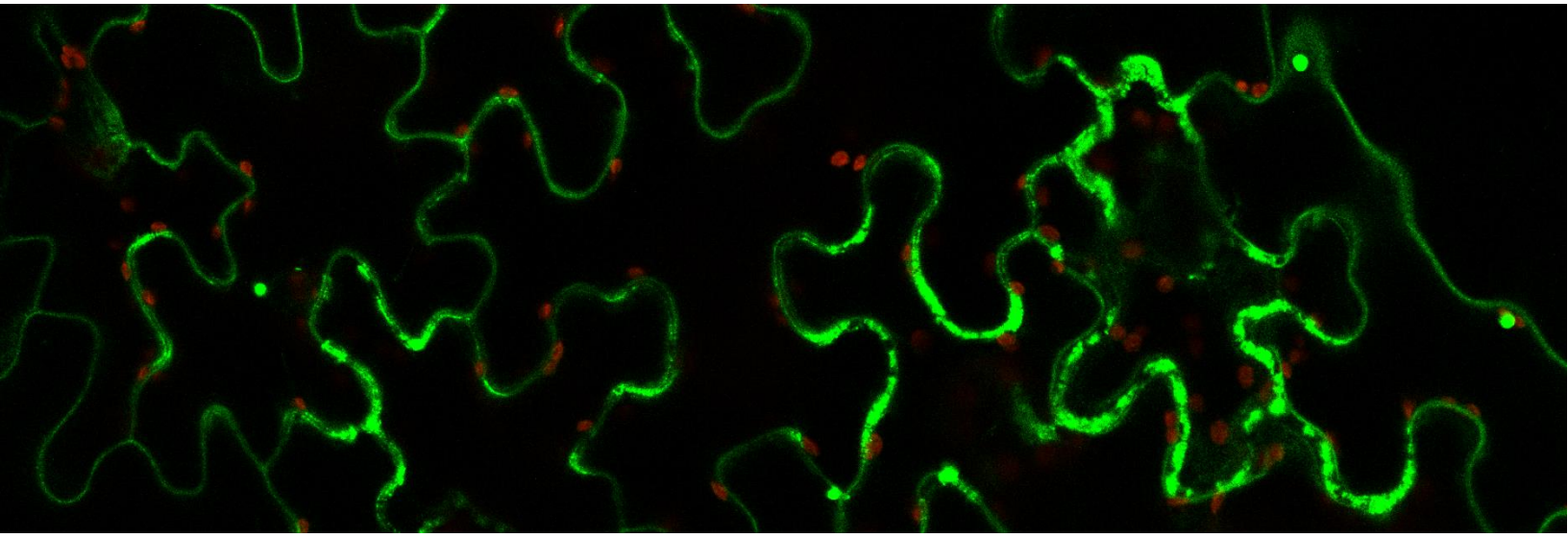

Development of Bimolecular Fluorescence Complementation reagents for the detection of *Arabidopsis thaliana* KAT1 protein-protein interactions using the GoldenBraid cloning system

Author: Alejandro Mossi Albiach

Tutor: Lynne Yenush

Bachelor's Degree in Biotechnology: Final Degree Project

Year 2015-2016

Valencia, 23rd May 2016

UNIVERSITAT POLITÈCNICA DE VALÈNCIA

ESCOLA TÈCNICA SUPERIOR D'ENGINYERIA AGRONÒMICA I DEL MEDI NATURAL

Author:

Student: Mr. Alejandro Mossi Albiach

Final Degree Project information:

Title:	Development of Bimolecular Fluorescence Complementation reagents for the detection of *Arabidopsis thaliana* KAT1 protein-protein interactions using the GoldenBraid cloning system
Venue:	Institute for Plant Molecular and Cell Biology (IBMCP)
Place and date:	Valencia, 23rd May 2016
Bachelor's Degree:	Bachelor's Degree in Biotechnology
Tutor:	Dr. Lynne Yenush

Keywords:

KAT1, BiFC, YFP, GoldenBraid, *Arabidopsis thaliana*

Abstract:

KAT1 is an *Arabidopsis thaliana* potassium voltage-gated channel of the Shaker family. This ion channel is fundamental for the control of membrane conductance in guard cells, leading to stomatal opening or closing in response to environmental changes. The stomatal movement controls the gas exchange, as well as the amount of water lost due to transpiration. Therefore, the underlying mechanisms of these stomatal movements will likely be influenced by proteins that regulate KAT1 activity.

The Shaker channels have been proposed to form functional channels associating into heterotetramers or homotetramers, but our knowledge regarding regulators of these potassium channels is very limited.

From a previous yeast-based high-throughput screening performed in our laboratory, a list of 14 possible KAT1 interacting proteins was obtained. To determine the physiological relevance of the identified interacting proteins, these interactions need to be confirmed in plant cells.

The Bimolecular Fluorescence Complementation (BiFC) technique is based on YFP's ability to recover its fluorescence upon physical approximation of its two halves. Using this technique, both the validity of the KAT1 interacting proteins and also the subcellular location of these interactions in the plant can be analyzed by confocal microscopy. GoldenBraid is a cloning system that allows the modular construction of multigenic DNA structures, and it provides a fast and efficient platform to assemble all the required pieces for the BiFC analysis and to insert them into a single multigenic construction. GoldenBraid is flexible enough to allow the construction of all desired fusion protein combinations. A well-established BiFC cloning procedure will be fundamental to study the protein-protein interactions of the candidate proteins because of the large number of possible combinations of fusion proteins required for these analyses (8 combinations for each interaction).

On the one hand, this project developed and implemented the KAT1 sequence as a GoldenBraid part and it was successfully tested in *Nicotiana benthamiana* using *Agrobacterium tumefaciens*-mediated transformation followed by confocal microscopy. And on the other hand, non-functional combinations for the BiFC assay were studied analyzing the expression and localization of KAT1-YFP and YFP-KAT1 fusion proteins which led to discard N-terminal fusions with KAT1.

Paraules clau:

KAT1, BiFC, YFP, GoldenBraid, *Arabidopsis thaliana*

Resum:

KAT1 és un canal de potassi regulat per voltatge d'*Arabidopsis thaliana* que pertany a la família Shaker. Aquest canal de ions és fonamental per al control de la conductància a la membrana de les cèl·lules guarda, causant l'obertura o el tancament dels estomes en resposta als canvis ambientals. El moviment dels estomes controla l'intercanvi de gasos, així com la perduda d'aigua per transpiració. Per aquesta raó, els mecanismes subjacents als moviments estomàtics estan probablement influenciats per les proteïnes que regulen l'activitat de KAT1.

S'ha proposat que els canals *Shaker* s'associen formant heterotetramers o homotetramers per tal de formar un canal funcional, però el nostre coneixement sobre els reguladors d'aquests canals de potassi és molt limitat.

A partir d'un cribratge d'alt rendiment basat en llevat realitzat al nostre laboratori, es va obtindré una llista de 14 possible proteïnes que interaccionen amb KAT1. Per tal de determinar la rellevància fisiològica de les possibles proteïnes que interaccionen amb KAT1, aquestes interaccions han de ser confirmades en cèl·lules vegetals.

La Complementació Bimolecular de Fluorescència (BiFC) és una tècnica basada en l'habilitat de YFP, que és capaç de recobrar la seva fluorescència per la aproximació de les seves dues meitats. Utilitzant aquesta tècnica, la validesa de les proteïnes que interaccionen amb KAT1 i també la localització subcel·lular d'aquestes interaccions en la planta podrà ser analitzada mitjançant microscòpia confocal. GoldenBraid es un sistema de clonatge que permet la construcció de manera modular d'estructures de DNA, i proporciona una plataforma ràpida i eficient per muntar totes les peces que es requereixen per a realitzar la BiFC i insertar-les en una sola unitat multigènica. El sistema GoldenBraid és suficientment flexible com per a permetre la construcció de totes les combinacions de proteïnes de fusió. Un protocol ben establert de BiFC serà fonamental per estudiar les interaccions proteïna-proteïna de les proteïnes candidates degut a l'elevat nombre de combinacions possibles de proteïnes de fusió que es requereixen per a aquests anàlisis (8 combinacions per a cada interacció).

Per un costat, aquest projecte ha desenvolupat i implementat la seqüència de KAT1 com a una part del GoldenBraid i va ser provada amb èxit en *Nicotiana benthamiana* utilitzant una transformació mitjançant *Agrobacterium tumefaciens* seguida del anàlisis per microscòpia confocal. I per altre costat, les combinacions no funcionals per a l'assaig de BiFC sigueren estudiades analitzant l'expressió i localització de les proteïnes de fusió KAT1-YFP i YFP-KAT1, fets que portaren a descartar les fusions N-terminals de KAT1.

Thank You

En primer lugar, por supuesto, quería agradecer a Lynne la labor que realiza conmigo y con todos los estudiantes que pasan por este laboratorio, ya que cada año hay que empezar desde cero con cada uno de nosotros y esto requiere dedicarnos tiempo y esfuerzo. Me has enseñado a pensar, a esforzarme, a ser mejor y a entender cómo se hace ciencia. Gracias.

Gràcies a la gent del laboratori, a Alba, que sempre estàs present i traus temps per atendre les nostres preguntes i dubtes. Gràcies a Ceci també, per ajudar sempre que ha sigut possible.

A ma Mare. Moltes gràcies per escoltar dia a dia els meus plans, els meus esquemes, la meua planificació i contribuir a millorar-ho tot. Moltes gràcies per creure sempre que puc més, ja que per això sé que res acaba ací i que queda molt per vindre. A mon pare, a Maria i a la "uela", gràcies per haver col·laborat i soportat la meua locura.

A Elisa, moltes gràcies per aguantar-me i per entendre'm, ja que sense tu, el camí haguera sigut molt més difícil. No puc imaginar com seria tot sense tu.

A Clara, mi "hallazgo biotecnológico", gràcies per haver aprés a donar-me la realitat a "pequeños sorbos", gràcies per la teua amistat incondicional.

Y por último, muchas gracias a Sergio y Teresa, que habéis resultado ser otro importante descubrimiento y espero que sigamos siempre unidos.

Index

Index of Figures

Index of Tables

Abbreviations

ABA	Abscisic Acid
Amp	Ampicillin
ATP	Adenosine TriPhosphate
ATPase	Adenosine TriPhosphatase
BiFC	Bimolecular Fluorescence Complementation
Cam	Cloramphenicol
cGMP	Cyclic Guanosine MonoPhosphate
DMSO	Dimethyl Sulphoxide
Gen	Gentamycin
GB	GoldenBraid
IPTG	Isopropyl β-D-1-thiogalactopyranoside
Kan	Kanamycin
K_{in}	Potassium Inward
K_v	Potassium Voltage-gated
LB	Lysogeny Broth rich medium for bacteria
OD	Optical Density
pα1_KAT1	pDGB3_alpha1+P35S+KAT1+Tnos
pα1_KAT1-YFP	pDGB3_alpha1+P35S+KAT1+YFP+Tnos
pα1_YFP	pDGB3_alpha1+P35S+YFP+Tnos
pα1_YFP-KAT1	pDGB3_alpha1+P35S+YFP+KAT1+Tnos
SNARE	Soluble N-ethylmeleimide-sensitive factor Attachment protein Receptor
Tet	Tetracycline
X-gal	5-bromo-4-chloro-3-indolyl-β-D-galactopyranoside
YFC	C-terminal fragment of the Yellow Fluorescent Protein
YFN	N-terminal fragment of the Yellow Fluorescent Protein
YFP	Yellow Fluorescent Protein

1. Introduction

1.1. The role of potassium in plants

Potassium is a key monovalent cation necessary for multiple aspects of cell growth and survival. This cation participates in numerous cellular functions, such as compensation of negative charges of macromolecules to maintain electroneutrality, cell turgor and volume, enzyme activity, protein synthesis and maintenance of proper membrane potential and intracellular pH. Generally, potassium is accumulated in cells against its concentration gradient to high amounts: cytosolic K^+ content may be within the 60-200 mM range and vacuolar K^+ content may arrive to 500 mM (Anschütz *et al.,* 2014).

In plants, potassium is an essential macronutrient, which can constitute up to 10% of the dry weight. Apart from the physiological functions listed above at the cellular level, this cation also plays a key role at the whole plant level, as it is involved in the control of stomatal movements that control water loss and desiccation (Anschütz *et al.,* 2014; Véry *et al.,* 2014).

1.1.1. Stomatal function

Water scarcity is one of the major stresses plants encounter and precisely for this reason many molecular, physiological and morphological mechanisms have been developed to cope with drought conditions. One of the most immediate and essential responses of the plants to water shortage is stomatal closure in order to minimize the water loss by transpiration. Therefore, advances in our knowledge regarding the molecular mechanisms underlying stomatal movements are likely to contribute to the development of plants that make a better use of water resources.

Stomata are microscopic openings found in the epidermis of the aerial parts of the plant. The stomatal pores are surrounded by a pair of guard cells which control the CO_2 and O_2 exchange with the atmosphere, and thus respiration and transpiration. Guard cell movements occur via reversible volume changes which are triggered by various environmental or endogenous signals (Anschütz *et al.,* 2014). Because of their autonomous character and their physiological importance, guard cells represent a particularly valuable and relevant model to study potassium transport across the plasma and vacuolar membranes (Assman and Wang, 2001). The manipulation of these ion fluxes, specifically those mediated by K^+ channels, have been proposed to represent promising targets for reverse engineering aimed to improve the stomatal response to diverse environmental conditions (Wang et al., 2014).

The variations in volume of the guard cells are produced by modifying the concentration of solutes that are present in the cytoplasm (Roelfsema and Hedrich, 2005). The flux of K^+, Cl^-, sucrose and malate across the guard cell membranes are the main contributors to the changes in volume of the guard cells driving stomatal aperture or closure (Schroeder *et al.,* 2001). The accumulation of ions and other solutes in the interior of the cell increase the osmotic pressure inside, diminishing the water potential which leads to the entrance of water into the cell by osmosis. The increase in cell volume causes the cells to bend and separate and this leads to the opening of the pore. On the contrary, ion release results in water going out of the cytoplasm and the guard cells decrease their volume, leading to closure of the stoma.

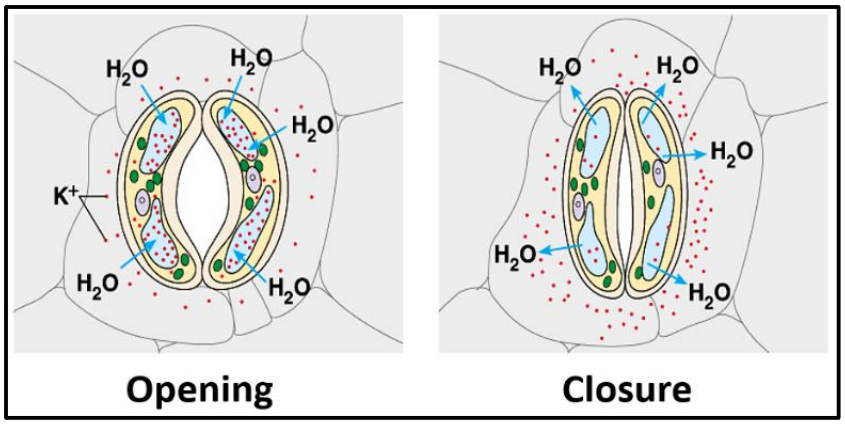

Figure 1.1. **Guard cell movements leading to stomatal opening and closing.** The osmotic pressure generated by K^+ intake generates the entrance of water into the cell, increasing the volume of the guard cells and provoking the opening of the stoma. On the other hand, the loss of water leads to a lower volume of the guard cells provoking the closure of the stoma, seen on 5th May, 2006. Image modified from http://bio100.class.uic.edu/lectf03am/guardcells02.gif.

The ion influx into the cell during stomatal opening is achieved by generating an outward proton flux mediated by the H^+- ATPase, which actively pumps protons outside of the cell. This extrusion of protons causes the hyperpolarization of the apoplast that leads to the activation of the voltage-gated potassium channels in the plasma membrane. K^+ uptake is balanced by the accumulation of anions such as Cl^-, $malate^-$ and NO_3^-. These fluxes contribute to the increase in the osmotic pressure, promoting the entrance of water into the cell (Schroeder *et al.,* 2001; Roelfsema and Hedrich, 2005).

The channels mediating the potassium flux in guard cells all belong to the K_v (potassium voltage-gated) family. In *Arabidopsis thaliana*, just a single gene, GORK, encodes a K^+ outward conducting channel (Hosy *et al.,* 2003), whereas for inward rectifying channels, five subunits have been identified: KAT1, KAT2, AKT1, AKT2/3 and AtKC1.

1.2. Shaker potassium channels: KAT1

Studies of plant genome sequences reveal 3 families of genes encoding plasma membrane K^+ transporters: the HKT family (Corratgé-Faillie *et al.,* 2010), the HAK/KUP/KT K^+ transporter family (Gierth and Mäser, 2007), and the Shaker K^+ channel family (Véry and Sentenac, 2003). The first two families can be identified in plants, fungi and bacteria, whereas the Shaker family is found in these organisms and also in animals.

The Shaker channels are similar with respect to their topology, containing 6 transmembrane (TM) segments and one pore region (P). Shaker-like K^+ channels seem to have their origin in a fusion of a gene encoding a 2 TM/1P channel and another gene coding for a voltage sensitive domain (VSD) (Figure 1.2 A). The latter consists of four transmembrane segments (4TM), and is a key element of voltage-gated ion channels required for sensing the transmembrane potential (Anschütz et al., 2014). In the case of plants, each Shaker channel is built of four α-subunits, with each subunit composed of 6 TM segments and 1 P domain (Figure 1.2 B). The C-terminal sequence of these transporters contain various regulatory elements (Latorre *et al.,* 2003; Sharma *et al.,* 2013).

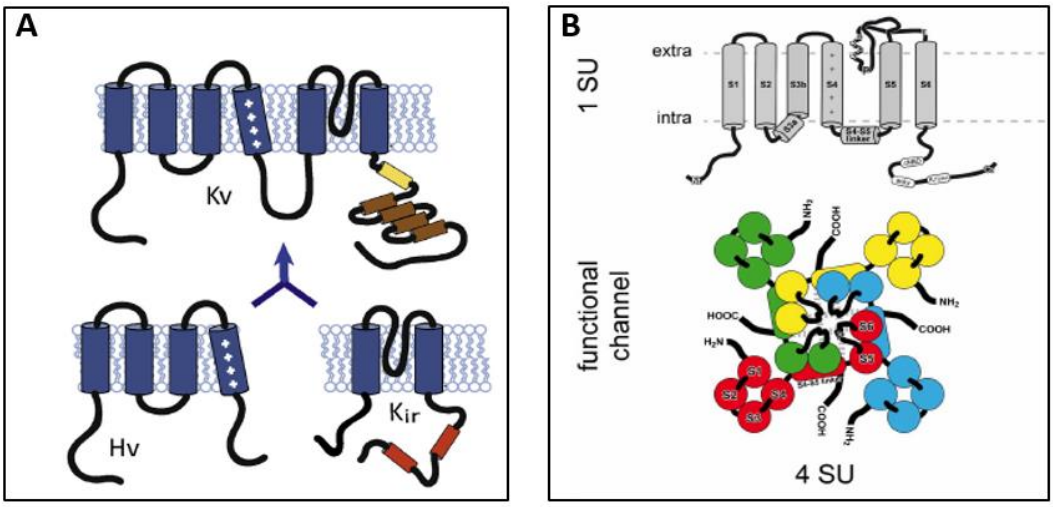

Figure 1.2. Origin, topology and structure of the Shaker-like K^+ channels. *A: The origin of Shaker-like K^+ channels might be the result of a fusion of a gene encoding 2TM/1P channel and another encoding a voltage sensitive domain (VSD) (image modified from Anschütz et al., 2014). B: Topology and structure of the Shaker-like K^+ channels with 6 transmembrane (TM) segments and 1 pore (P) domain. The lower panel shows the tetrameric organization (image modified from Sharma et al., 2013).*

Arabidopsis contains 9 members of the Shaker channel family which can be classified into 5 different groups based on both phylogeny and functional aspects (Pilot *et al.,* 2003). Two of these groups contain 5 inward rectifying channels: AKT1, AKT6, SPIK, KAT1 and KAT2. All of the channels in these two groups are considered to be K^+-selective voltage-gated channels and dominate the membrane conductance in most cell types, including the guard cells. Based on the structural data obtained from bacterial and animal Shaker channels, this family has been proposed to adopt tetrameric pore forming structures, which can be composed of homo or heterotetramers (Figure 1.2 B) (Jiang et al., 2003; Long et al., 2005). Among these shaker channels, KAT1 has been proposed to be the dominant K_{in} channel in guard cells (Nakamura *et al.*, 1995).

The KAT1 channel is the best studied member regarding structure and function, and it wasthe first potassium channel to be molecularly characterized (Anderson *et al.,* 1992). As a member of the K_V channel family, KAT1 contains 6 TM segments (Uozumi *et al.,* 1998). The first four TM segments act as the Voltage Sensing Domain and the positive charges in the 4th TM segment play an important in channel conductivity (Figure 1.3 A) (Sharma *et al.,* 2013). The voltage sensitivity of guard cell inward rectifying channels has been related to a histidine residue. However, mutations of the histidine residue in KAT1 do not affect its pH dependence. It has been proposed that a region with different sensing amino acids, termed a sensory cloud, would be involved in the acid activation mechanism rather than a single amino acid (Gonzalez *et al.,* 2012). In addition, the long cytosolic C-terminus tail of KAT1 has been shown to play an important role in the modulation of this potassium channel. The sequence contains a cNBD domain (cyclic nucleotide binding domain) (Figure 1.3 B) that has been reported to be modulated by ATP and cGMP. While cGMP binding reduces KAT1 currents, ATP affects KAT1 positively (Hoshi, 1995).

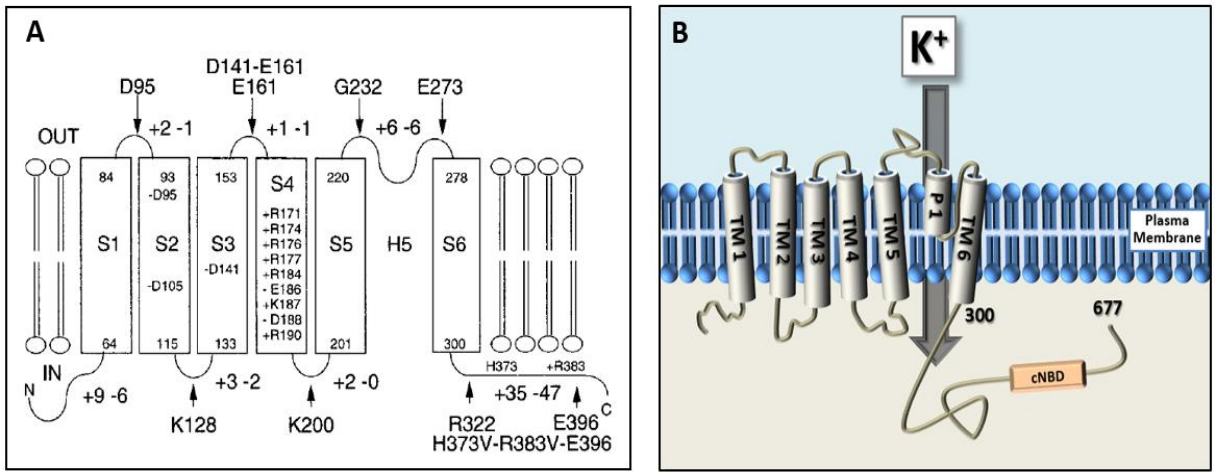

Figure 1.3. Topology of the KAT1 channel. *A: Detailed topology of the transmembrane segments of the KAT1 channel, information regarding the tansmembrane (TM) segments and functionally relevant amino acids depicted (image from Uozumi et al., 1998). B: description of the complete KAT1 topology (TM segments and Pore (P) domain) and cytosolic tail with a cNBD (cyclic nucleotide binding domain).*

As is the case with all Shaker family channels studied to date, KAT1 has also been proposed to form tetramers. The sequences or sequences mediating this tetramerization have yet to be defined; however, it is known that KAT1 can form homotetramers or heterotetramers with the other members of the Shaker channel family, KAT2, AKT1 and AKT2. The KAT2 channel shares a great degree of homology with KAT1. More specifically, these two transporters share 88% identity in the first 500 amino acids, while in the last 177 amino acids, the level of conservation drops to 45%. Both have been shown to play an important role controlling stomatal opening. However, KAT1 is not strictly required to carry out this function in some Arabidopsis ecotypes, indicating that redundancy among homo and heterotetramers must exist (Jeanguenin *et al.,* 2011). In addition to KAT2, AKT1 and AKT2, it has been suggested that two other proteins, AtKC1 and KAB1 can participate in the formation of heterotetramers. In the case of AtKC1, it does not appear to have its own intrinsic transporter activity, but co-expression in *Xenopus* oocytes of the AtKC1 subunit with these other channels has shown that they functionally interact (Jeanguenin *et al.,* 2011). It is speculated that KAB1, which is a putative homolog of animal K^+ channel β-subunit, is capable of stabilizing and enhancing the transport capacity of the protein complex formed with KAT1, again using the *Xenopus* oocyte model (Zhang *et al., 1999*).

As a key component of potassium fluxes in guard cells and other tissues, the regulation of KAT1 in the context of homo or heterotetramers is predicted to be complex. For example in addition to the intramolecular regulatory elements and the hetertetramerization discussed above, several proteins have been shown to physically and/or functionally interact with KAT1. For exemple, the KAT1 channel has been suggested to bind to and be activated by 14-3-3 proteins (Sottocornola *et al.,* 2008; Sottocornola *et al.,* 2006). These proteins have been reported to modulate the KAT1 channel in *Xenopus* oocytes, shifting the required voltage to activate KAT1. Although, the mechanism by which these proteins are able to control the voltage dependency of KAT1 is still unknown, it has been proposed to involve 14-3-3 proteins binding to phosphorylated residues of KAT1. This hypothesis suggests that KAT1 and possibly KAT2 could be modulated by phosphorylation. In support of this hypothesis, at least two classes of protein kinases have been implicated in the regulation the KAT1 channel. For example, the Open Stomata 1 (OST1), a SNF-1

related kinase involved in Abscisic Acid (ABA) signaling, has been shown to phosphorylate KAT1 at threonines 306 and 308. Although no function for the modification of Thr^{308} has been observed, the modification of Thr^{306} reduces the K^+ uptake activity of KAT1 (Sato *et al.,* 2009). More recently, KAT1 (but not KAT2) was shown to physically interact with OST1, adding support to the physiological relevance of this regulatory mechanism (Acharya *et al.,* 2013).

The second class of kinases proposed to modulate the activity of the KAT1 channel is the calcium-dependent protein kinases. It has been proposed that the phosphorylation recognition sequence of the plant calcium-dependent kinases resembles the sequence of animal protein kinase C. KAT1, expressed in *Xenopus* oocytes, has been reported to be inhibited by the protein kinase C activator phorbol 12-myristate 13-acetate (Sato *et al.,* 2010). In addition, KAT1 and KAT2 have been shown to be phosphorylated and inhibited by CPK13, which is a member of the Ca^{2+} dependent protein kinases (CPK) family (Ronzier *et al.,* 2014). However, in both cases, the mechanisms by which these phosphorylation events regulate potassium transport activity are still unknown.

The phytohormone, abscisic acid (ABA) controls ion transport and transpiration in plants under water stress. Interestingly, ABA treatment triggers the selective endocytosis of the KAT1 potassium channel proteins in the epidermal guard cells. It initiates the endocytosis and sequestration of these receptors within an endosomal membrane pool that recycles back to the plasma membrane within hours (Sutter *et al.,* 2007). The signaling pathway mediating this response is largely undefined. However, as mutants lacking the Ost1 are no longer sensitive to channel inhibition mediated by ABA, this kinase is likely to play an important role (Acharya *et al.,* 2013). In addition, a member of the SNARE (soluble N-ethylmaleimide-sensitive factor attachment protein receptors) family of proteins, AtSyp121 has been implicated in the anchoring and distribution of the KAT1 channel within the plasma membrane (Sutter *et al., 2006*). AtSyp121 acts in late in secretory pathways to the plasma membrane, and the disruption of its activity affects the secretory pathway and the protein traffic, and suppresses the regulation by ABA of the guard cell K^+ and Cl^- channels (Leyman *et al.,* 1999) . It has been also shown that the KAT1 channel is able to interact with VAMPs (vesicle-associated membrane proteins) that in *Arabidopsis* have been related to ABA-mediated stomatal closure. More specifically, $VAMP_{721}$ and $VAMP_{722}$ were reported to interact with the KAT1 channel (Zhang, 2015). However, the mechanism by which these proteins regulate KAT1 transporter activity in response to ABA treatment is still unclear.

As discussed above, KAT1 has become an interesting model to study the Shaker-like K^+ channels because it is a highly regulated protein that can be studied at many levels. However, the molecular processes underlying the modulation of this protein are still largely unknown. Therefore the discovery of new proteins that participate in the regulation of KAT1 may help to define mechanisms of regulation and identify potential targets that impact stomatal movements. In our laboratory, the yeast *mating-based Split-Ubiquitin* system was used to identify 14 possible KAT1 interactors from an *Arabidopsis thaliana* cDNA library. The next step in this analysis, and the focus of the present study, is the confirmation of these interactions in plant cells. In order to achieve this, the Bimolecular Fluorescence Complementation system has been chosen to analyze KAT1 interaction proteins in *Nicotiana benthamiana*.

1.3. The Bimolecular Fluorescence Complementation (BiFC) system

Protein-protein interactions are basic cellular events inherent to every physiological process and occur in all subcellular compartments. The identification of interacting protein partners provides insight into the regulatory networks that take place inside the cells and gives clues about the physiological role of proteins. Several techniques have been developed for the identification and

characterization of such protein-protein interactions *in vitro* or *in vivo*. Co-immunoprecipitation and genetic methods, such as the yeast two-hybrid system, are among the most widely used techniques.

More recently, a novel approach termed biomolecular fluorescence complementation (BiFC) has been developed as one of the most advanced and powerful tools for studying protein-protein interactions in living cells. The BiFC assay is based on the observation that two non-fluorescent fragments of a fluorescent protein can associate to reconstitute the functional fluorescent protein. Furthermore, the association of these fragments can be facilitated by fusing them to two proteins that interact with each other, so the non-covalent association of the fragments produces the biomolecular fluorescent complex. Many of the interactions can be identified even when the fusion proteins are expressed at concentrations similar to those of their endogenous counterparts. The BiFC technique has been applied to study protein-protein interactions between different types of proteins and in a wide range of cellular locations in different organisms, including several plant species (Citovsky *et al.,* 2006). Moreover, the BiFC system has been particularly valuable for the visualization of membrane protein interactions because of the potential role of the membrane environment in controlling the formation of the complex (de Virgilio *et al.,* 2004; Hynes *et al.,* 2004). For example, the BiFC system has been used to identify and characterize the interactions among components of signal transduction routes, such as the TGF-β signaling pathway (Remy *et al.,* 2004). Therefore, the BiFC system is suitable for the detection of KAT1 interaction with its candidates in plant cells.

In the BiFC assay, the fluorescent protein, Yellow Fluorescent Protein (YFP) in this case, is split into two portions, N-terminal (YFN) and C-terminal (YFC), neither of which fluoresces on its own. When the two fragments come within close proximity they non-covalently interact reconstituting the functional YFP protein (Figure 1.4).

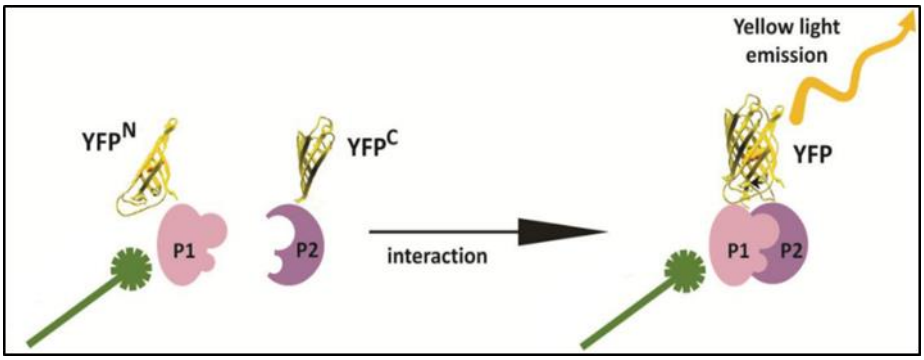

Figure 1.4. Schematic diagram representing the principle of the BiFC assay. *The two fragments of the YFP protein are fused to two putative interacting proteins (P1 and P2). The interaction of proteins P1 and P2, reduces the distance between the two YFP fragments, so that they are able to associate and reconstitute YFP, and the fluorescence is reconstituted (image modified from Horstman et al., 2014).*

One factor that influences the ability to detect these protein-protein interactions using the BiFC assay is the effect of the YFP fusions on the protein of interest. Protein-protein interactions are mediated by specific protein domains and the fusion of other proteins may alter the ability of these domains to interact or lead to misfolding, which would prevent the interaction or even lead to the degradation of the protein (Bracha-Drori *et al.,* 2004). Therefore, to exclude false negative combinations that could lead to the erroneous conclusion that there is no interaction, all possible combinations of constructs must be tested (Kerppola, 2006). There are eight possible combinations, in which YFN and YFC are fused to the N-terminus and C-terminus of the proteins of interest (Figure 1.5).

Another aspect that must be taken into consideration is the effect of the chosen peptide linker placed between the protein of interest and the YFN/YFC fragment. It has been proposed that the length and sequence of the linker peptide between the YFN/YFC fragment and the protein could affect the ability of these fragments to reassemble and reconstitute the fluorescent protein. This linker could interfere with the BiFC assay affecting the flexibility and three-dimensional structure of the fusion protein (altering its natural folding) (Arai *et al., 2001*). However, other authors have suggested that the role of the linker peptide is important, but not critical for the success of a BiFC experiment (Horstman *et al.,* 2014).

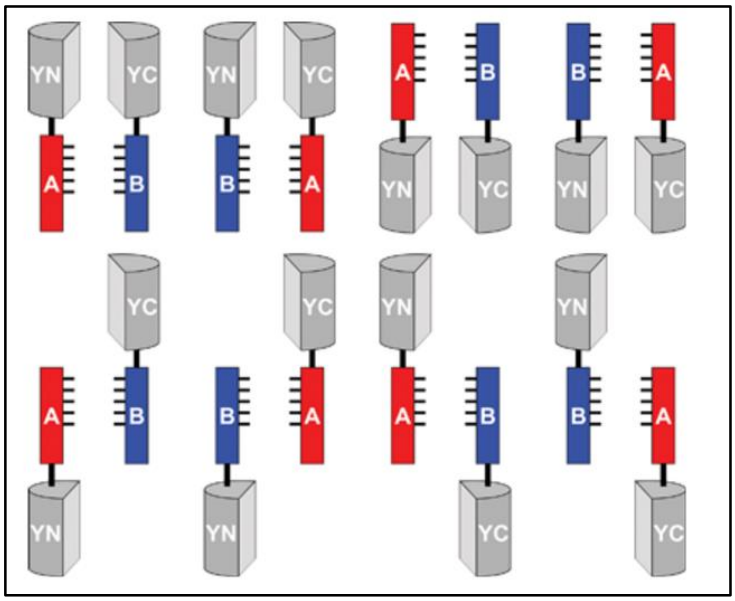

Figure 1.5. Combinations of fusion proteins to be tested for BiFC. *The combination of the fusion proteins that result in a positive interaction in the BiFC must be found empirically. This image shows the eight possible combinations of fusion proteins in order to perform the BiFC assay in which YFN and YFC fragments can be fused either to the N-terminus or the C-terminus of the tested proteins (image from Kerppola, 2006).*

The aim of the current project is to generate reagents that can be used to test KAT1 protein-protein interactions with the 14 candidate proteins. As discussed above, many combinations of constructs must be tested in each case. Therefore, we have chosen to carry out these experiments using the GoldenBraid modular cloning strategy, which will be described in detail below.

1.4. GoldenBraid cloning system for transient expression in *Nicotiana benthamiana*

GoldenBraind (GB) is a modular assembly system that allows the binary combination of multipartite assemblies that can be used for the construction of plasmids with up to 6 transcriptional units. GB uses the Golden Gate cloning method to generate a molecular assembly of standardized basic parts, which are the incorporated to a double loop (“braid”) cloning design, enabling the standardization of Golden Gate for its use in synthetic biology (Sarrion-Perdigones *et al.,* 2011). The systematic, modular and standardized nature of GB makes this cloning system the most suitable option to perform the proposed BiFC assays. This system facilitates the construction of the desired fusion proteins and allows for the generation of the different BiFC partner combinations in the same plasmid. This is a particular advantage in that it essentially guarantees that both fusion proteins will be expressed in each transformed cell. If traditional BiFC vectors were to be used (each construct in separate plasmids), during the transformation many cells may have only one of the two plasmids, thus decreasing the efficiency of the analysis.

The assembly strategy of the GB system can be described using a language analogy in that the hierarchical manner in which the different building blocks in GB are combined to form a multigenic structure are reminiscent of grammar elements (morphemes, words, phrases). The process used for the construction of a final GB multigenic construct from the most basic GB units is depicted in Figure 1.6 A. Thus, the first step consists in the design of the minimal GB parts which are the DNA sequences that are to be included in the final construct. These GB parts are fragments of DNA flanked by four nucleotide overhangs that will confer a specific position within the final construct (see below). The GB parts are stored as inserts within a designed entry vector (pUPD), from which they will be released by cleavage with restriction enzymes (Sarrion-Perdigones *et al.,* 2013). Then, the GB words (GB parts) are assembled generating a higher order organization (superpart) depicted in Figure 1.6 A. These pieces are promoters, coding sequences, terminators, N-terminal fusions, C-terminal fusions and so on. The assembly of superparts and/or parts will generate the transcriptional unit (TU). This standardized GB grammar with parts and superparts is shown in Figure 1.6 B.

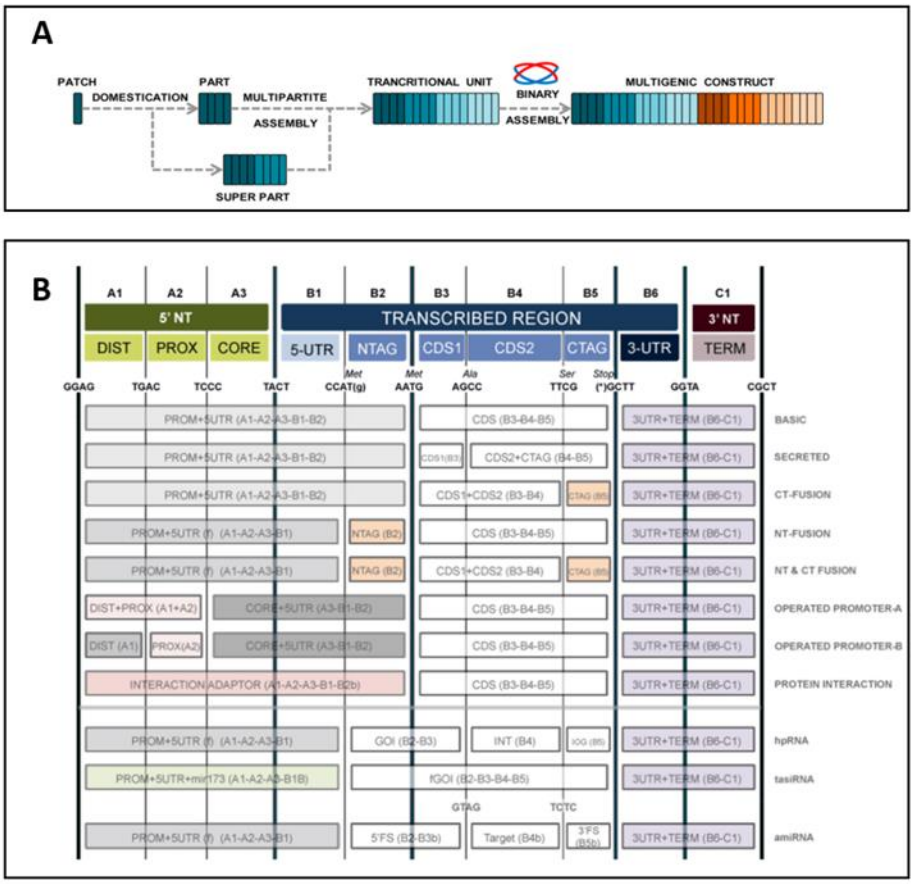

Figure 1.6. GoldenBraid cloning system process and grammar. *A: Scheme of the process for the production of a multigenic structure: The multipartite assembly of the GB parts/superparts leads to the formation of a transcriptional unit, and using binary assembly, different transcriptional units may be assembled into a multigenic construct (image modified from Sarrion-Perdigones et al., 2013). B: GoldenBraid grammar 3.0 which shows the different overhangs that the parts/superparts must have in order to be properly inserted into the transcriptional unit, seen 6th May, 2006. Available at https://gbcloning.upv.es/do/multipartite/.*

In order to adapt the desired sequences with the corresponding overhangs, i.e., transform them into GB parts, they must be "domesticated", or in other words, adapted to the GB grammar.

The GB domestication is performed by amplification of the target sequence (to produce a GB part or superpart) using specific primers in a PCR reaction that allows for the introduction of the generated fragment into a pUPD vector by means of a *BsmBI* digestion-ligation. The domestication protocol may require the elimination of internal *BsmBI* and *BsaI* restriction sites. In this case, the production of smaller units in the GB grammar, called GB patches is required. The elimination of the internal recognition sites is done by substituting the original sequence with one that eliminates the recognition site, but does not alter the protein sequence. GB patches are reassembled in a single-tube *BsmBI* digestion-ligation reaction into the pUPD to produce the new GB part or superpart (Figure 1.6 A).

As mentioned, the GB cloning technique is based on the use of two restriction enzymes: *BsaI* and *BsmBI*. Both are type IIS restriction enzymes. Both enzymes cut downstream and outside the recognition site and leave a 4 nucleotide overhang. This overhang sequence is completely independent of the recognition site and it confers each piece with a specific position inside of the transcriptional unit. As these enzymes cut downstream of the recognition site, the restriction site disappears resulting in a permanent junction that no longer includes the recognition site. The four base pair overhangs are designed to mediate the assembly of the different pieces based on sequence complementarity that allows for their binding and ligation in the restriction-ligation reactions (Figure 1.7).

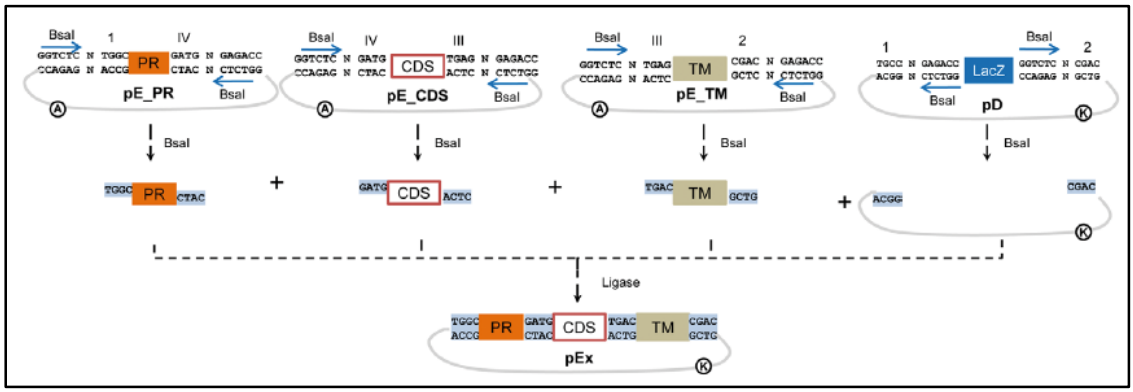

Figure 1.7. Multipartite assembly of different part/superparts into a transcriptional unit. *GB parts/superparts present in an entry plasmid, pUPD, are released and assembled with a BsaI digestion-ligation reaction. Arabic and latin numbers indicate how the parts will rearrange constituting the final transcriptional unit within a destination vector (image from Sarrion-Perdigones et al., 2013).*

GB destination vectors (pDGBs) are binary vectors that function as recipients of new assemblies. There are two levels: α and Ω. Standard parts are normally assembled into a level α plasmid using a *BsaI* digestion-ligation, as shown in Figure 1.7. Then transcriptional units can be assembled into a multigenic construct by moving to an Ω level plasmid using a *BsmBI* digestion-ligation. Moving back and forth between α and Ω plasmids, different TUs are assembled increasing the multigenic construction (Figure 1.8).

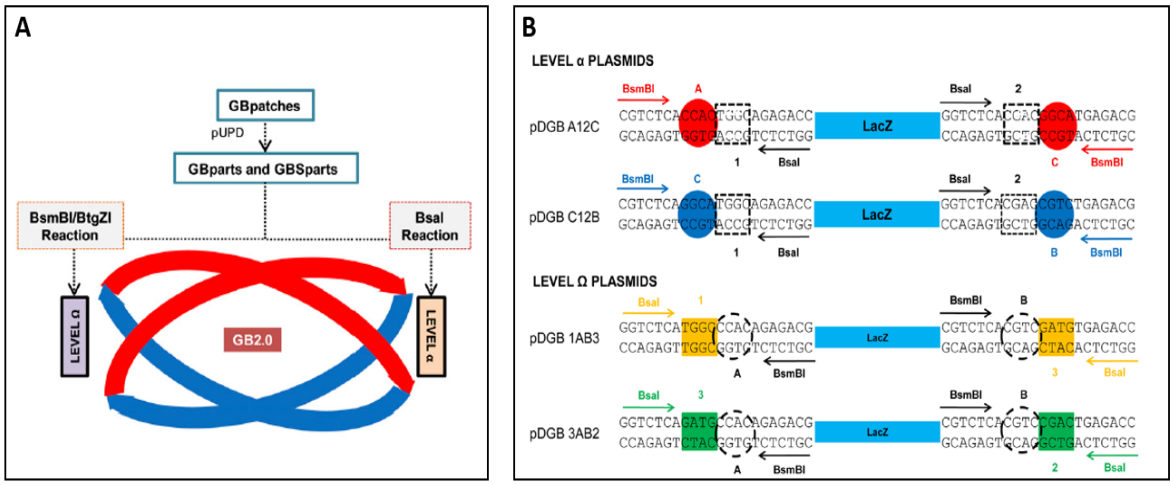

Figure 1.8. Scheme of the GoldenBraid cloning process and α and Ω level plasmids. *A: Scheme of the GoldenBraid cloning procedure, highlighting the double braid (image modified from Sarrion-perdigones et al., 2013). B: Schematic representation of the α and Ω level plasmids. The overhangs and enzymes used for each type of plasmid are shown (image from Sarrion-Perdigones et al., 2013).*

Importantly, the α and Ω level plasmids of the GoldenBraid system are integrated into the pCambia binary vector, which has been routinely used for *Agrobacterium tumefaciens*-mediated transformation of several plant species (Roberts *et al.,* 1998). Therefore, the vectors generated using this system are perfectly suited to perform the proposed BiFC assays in *Nicotiana benthamiana* plants using standard transient transformation protocols.

The aim of this project is to generate tools to carry out BiFC protein-protein interaction studies between KAT1 and the 14 candidate proteins previously identified in our laboratory. As explained above, a considerable number of constructions will be required to carry out these analyses. It is important to note that KAT1 is a transmembrane protein and in order to properly design BiFC experiments, its structure must be taken into consideration. As described above, both the N-terminus and C-terminus of KAT1 are in the cytosol, so potentially the transporter could interact with proteins at both ends. However, the fusion of YFN/YFC might alter the localization of the protein, the delivery of the protein to the plasma membrane or it may even be processed with the signal peptide during membrane insertion and not be present in the mature form of the transporter. Therefore, in addition to the initial domestication of the KAT1 coding sequence, we will carry out studies of the functionality of N-terminal and C-terminal fusions of the entire YFP protein to the KAT1 coding sequence using the GoldenBraid cloning system. These studies are essential first steps for the design and execution of the proposed BiFC assays

2. Objectives

The main objectives proposed for this work are as follows:

1. The domestication of the KAT1 sequence as GB part which is able to be integrated into a whole transcriptional unit using the GoldenBraid cloning system.
2. The development of the working protocol and reagents to perform a BiFC assay to analyze KAT1 protein-protein interactions in *Nicotiana benthamiana.*
3. The functional analysis of YFP-KAT1 and KAT1-YFP fusion proteins to determine the effect of an N-terminal and a C-terminal fusion with KAT1.

3. Materials and Methods

3.1. Biological material and growth conditions

3.1.1. *Escherichia coli*

For the construction and amplification of the plasmids the DH5α *E. coli* strain was used. The employed medium was the Lysogeny broth (LB), containing tryptone (1%), yeast extract (0.5%) and sodium chloride (1%). Depending on the resistance gene included in the plasmid, the media was supplemented with several different antibiotics: 50 μg/mL Ampicillin (Amp), 50 μg/mL Kanamycin (Kan), 25 μg/mL Chloramphenicol (Cam), 25 μg/mL Gentamycin (Gen) and/or 5 μg/mL Tetracycline (Tet).

When required for the preparation of a solid medium, 2% agar was added. Cells were cultivated at 37°C for 24 hours.

In order to identify the cells containing the correct plasmid constructed using GB, a blue-white screening was performed. The blue-white screening is a rapid and efficient technique for the identification of recombinant bacteria that relies on the activity of the β-galactosidase enzyme that cleaves lactose into glucose and galactose. For screening the clones containing recombinant DNA, a chromogenic substrate known as X-gal (5-bromo-4-chloro-3-indolyl-β-D-galactopyranoside) is added to the agar plate and if β-galactosidase is produced X-gal is hydrolyzed to form 5-bromo-4-chloro-indoxyl that suffers a spontaneous dimerization producing an insoluble blue pigment 5,5'-dibromo-4,4'-dichloro-indigo. IPTG (isopropyl β-D-1-thiogalactopyranoside) is used along with X-gal in the blue-white screening since it is a non-metabolizable analog of galactose that induces the expression of the LacZ gene. The solid media was supplemented with 40 μg/ml X-gal and 0.5 mM IPTG. The plasmids incorporating the gene of interest into the vector lose the LacZ gene so that they do not metabolize the X-gal and produce white colonies which are the selected ones; the cells that contain the empty plasmid maintain the LacZ gene, and so encode for β-galactosidase, which will transform the X-gal substrate and develop a blue color. These transformants are discarded.

3.1.*2. Agrobacterium tumefaciens*

For the transient transformation of *Nicotiana benthamiana* with plasmids generated using GB 3.0, the *Agrobacterium tumefaciens* strain GV3101::pMP90 was used since this strain has provided successful results in plant transformation (Clough *et al.,* 1998). *A. tumefaciens* strain GV3101::pMP90 contains the genetic background C58 which confers a natural resistance to Tet and also contains the Ti (tumor inducing) plasmid pMP90, which confers the Gen resistance and has the Vir region. Genes in the Vir region are grouped into the operons VirABCDEFGH. These Vir genes are responsible of translating the activation signal for transformation and transport the DNA fragment into the *N. benthamiana* cells.

The employed media was LB supplemented with the corresponding antibiotics: Tet, Gen and Kan (for the GoldenBraid α plasmid selection).

The cells were grown at 28°C for 48 hours.

3.1.3. *Nicotiana benthamiana*

Nicotiana benthamiana plants were used for the agroinfiltration experiments to perform the protein expression and subcellular localization analysis by means of confocal fluorescence microscopy. Plants were grown from the seeds under controlled conditions (23 °C and 70% relative

humidity) and a long-day photoperiod (16 hr light and 8 hr dark, with illumination of 70 µE m^{-2} sec^{-1}) for 4 weeks. The plants were grown in square polystyrene flowerpots 7x7x8cm with a mixture of exfoliated vermiculite ("Verlite", Vermiculita y exfoliados S.L.) and peat (Profisubstrat Gramoflor Vertriebs) (1:1 v/v).

3.1.4. Promoter, terminator, protein coding genes and vectors

The chosen promoter was the *Cauliflower mosaic virus* (CaMV) 35S promoter (P35S) since it has been previously shown to produce a stable, high-level expression of proteins in *Agrobacterium*-mediated transient expression in *Nicotiana spp* (Petrie *et al.,* 2010; Sarrion-Perdigones *et al.,* 2011; Sarrion-Perdigones *et al.,* 2013). For the same reasons the terminator nos (Tnos) was chosen (Sarrion-Perdigones *et al.,* 2011; Sarrion-Perdigones *et al.,* 2013). The sequences were obtained from plasmids from the GB collection of Dr. Diego Orzáez's laboratory. Their IDs are: GB0030, GB0552, and GB0037; and are found in the https://gbcloning.upv.es database.

The YFP sequence used as the template for the cloning procedures described here was from the GB plasmid GB0053.

Finally, the vector KAT1-pMetYCgate obtained from the Arabidopsis Biological Resource Center (ABRC CD3-815) was used as the template for the construction of the AtKAT1-containing plasmids using the primers described in Figure 4.2 and following the procedure explained in section 3.3.1 of Materials and Methods.

The vectors used to perform the GB 3.0 experiments were the domesticator vector that contains a Cloramphenicol resistance gene, and the level α destination vector which is a GB adapted version of the pCambia binary vector and contains a Kanamycin resistance gene. Their IDs are: pUPD2 and pDGB3_alpha1 respectively (annex). Both vectors contain the LacZ gene which is released during the digestion-ligation reaction allowing for the blue-white screening described above.

3.2. Genetic Transfer Techniques

3.2.1. Plasmid Extraction

The cells containing the plasmids of interest were grown in liquid LB culture with the corresponding antibiotic and were incubated overnight at 37°C in agitation.

Plasmids extraction was performed using the *NucleoSpin Plasmid EasyPure* (Machery-Nagel). This plasmid extraction is based on a column purification of the plasmidic DNA after an alkaline lysis. The protocol starts from cells contained in a 5 mL saturated pre-culture collected by centrifugation at maximum speed. After discarding the supernatant the pellet is resuspended in 150 µL of the *A1 Buffer*. After that, 250 µL of the *A2 Lysis Buffer* are added, mixed by inversion and left at room temperature for 2 minutes. This is followed by 350 µL of the *A3 Neutralization Buffer* and inversion until loss of color, followed by a 3 minute centrifugation at 15700 *g*, and the obtained supernatant is poured into the column and centrifuged for 30 seconds at 1800 *g*, the flow through is discarded. After that, 450 µL of the *AQ Washing Buffer* is added to the column and centrifuged for 60 seconds at 15070 rcf. Finally, the plasmid is obtained adding 60 µL of the *AE Elution Buffer* to the column and collecting the eluate by centrifugation at 15700 *g*.

After the purification the amount of DNA was quantified measuring the absorbance at 260nm.

3.2.2. *E. coli* transformation

E.coli was transformed by heat shock, using 5 µL of the digestion-ligation reaction product (see section 3.3.2). 100 µL of *E. coli* competent cells were mixed with the digestion-ligation product and kept at 4°C for 30 min. The mixture was then incubated at 42°C for 30-60 seconds and then returned to 4°C. 600 µL of LB was added and the sample was incubated for 45-60 min at 37°C in agitation. Finally, 600 µL were plated onto LB plates with the corresponding antibiotic and reagents for the blue-white screening.

3.2.3. Agrobacterium tumefaciens transformation

Competent *A. tumefaciens* GV3101::pMP90 cells were made using the following protocol: a 50 mL culture was grown in LB with Tet (5 µg/mL) and Gen (25 µg/mL) at 28°C until an OD_{600} of 1.0. The cells suspension was centrifuged at 1800 *g* during 15 minutes and the pellet was resuspended in 1 mL of 20 mM $CaCl_2$, divided into 0.1 mL aliquots and finally stored at -80°C in liquid nitrogen until the use.

The desired constructions were introduced into the *A. tumefaciens* strain GV3101::pMP90 following a modified protocol of the freeze-thaw method (Holsters *et al.,* 1978). A 0.1 mL aliquot of competent cells was thawed and 1 µg (aprox. 10 µL) of the corresponding plasmid was added, the mixture was rapidly frozen in liquid N_2 and then incubated at 37°C for 5 minutes. Then, 0.9 mL of LB + Tet + Gen was added and the sample was incubated for 4 hours at 28°C with slow agitation. Finally the suspension was plated onto LB plates containing Tet, Gen and Kan (for the vector containing the desired construction) and 1.5% of Pronidase agar. Plates were incubated in the dark at 28°C and the colonies resistant to the antibiotics appeared in 2-3 days.

3.2.4. *Nicotiana benthamiana* transformation

N. benthamiana leaves were transformed by injection of *A. tumefaciens* GV3101::pMP90 cells harboring the appropriate plasmids as follows: to suppress gene silencing *A. tumefaciens* cells expressing the p19 protein of the Tomato Bushy Stunt virus from *Plant Bioscience Limited* (PBL, Norwick, UK) are used in the co-infiltration protocol. Overnight cultures of *A. tumefaciens* of approximately 2.0 OD_{600} units were collected and resuspended in a similar volume of infiltration buffer (10 mM $MgCl_2$, 10 mM MES pH 6.5, 200 µM acetosyringone) and incubated at 28°C for 3 to 4 hours. A mixture of *A. tumefaciens* strains containing the fluorescent fusion construct and the p19 plasmid was prepared —at OD_{600} 1.0 the cultures were mixed using two volumes of the culture with the desired constructions and a volume of the p19 culture. This 2:1 mixture was used for co-infiltration into the abaxial air space of *N. benthamiana* leaves with a needleless syringe. Approximately 1 mL of the *Agrobacterium* mixture was used for each site of infiltration and each infiltration was performed at least in triplicate for each time point.

Epidermal cell layers of at least two transformed leaves of 2-3 plants of similar age were assayed for fluorescence using confocal microscopy at 24, 48 and 72 hours post-infiltration, and the same assay was done twice.

3.3. Plasmid construction using GoldenBraid 3.0

3.3.1. PCR conditions

The domestication started with an amplification by PCR. Table 3.1 shows the different reagents employed:

Table 3.1. Reagents used in the amplification by PCR. *The polymerase employed was the High fidelity Phusion (Thermo Scientific).*

	PCR reaction
DNA	1µl (1ng approx.)
Oligo Fw (10 µM)	0.5 µl
Oligo Rv (10 µM)	0.5 µl
dNTPs (2 mM)	1 µl
Buffer GC 5X	5 µl
DMSO	0.5 µl
Phusion Taq (2 U/µl)	0.5 µl
H_2O	16 µl
Final Volume	25 µl

The PCR conditions used for each KAT1 patch are shown in Table 3.2. As shown patch 1 and 2 were obtained using the same thermic profile, while patch 3 amplification for B3B4 and B3B4B5 had to be performed with different thermic profiles.

Table 3.2. PCR conditions used for the amplification of the different KAT1 patches. *High Fidelity Phusion polymerase is able to extend 2kb per minute, so that both versions of patch 3 required 30 seconds of amplification while 20 seconds was sufficient for patch 1 and 2.*

	KAT1-P1		**KAT1-P2**		**KAT1-P3 B3B4**		**KAT1-P3 B3B4B5**	
Number of Cycles	T (°C)	Time	T (°C)	Time	T (°C)	Time	T (°C)	Time
1	98	5'	98	5'	98	5'	98	5'
35	98	20''	98	20''	98	20''	98	20''
	54	30''	54	30''	51	30''	49	30''
	72	20''	72	20''	72	30''	72	30''
1	72	7'	72	7'	72	7'	72	7'

The PCR conditions used for both YFP pieces are shown in Table 3.3.

Table 3.3. PCR conditions used for the amplification of YFP.

	YFP-Linker B2		**Linker-YFP B5**	
Number of Cycles	T (°C)	Time	T (°C)	Time
1	98	5'	98	5'
30	98	20''	98	20''
	57	30''	59.5	30''
	72	30''	72	30''
1	72	7'	72	7'

3.3.2. Digestion-ligation reactions

The digestion-ligation reagents are indicated in Tables 3.4 and 3.5. These digestion-ligation reactions consisted of 50 cycles, with each cycle containing a step at 37°C for 2 minutes and a second step at 16°C for 5 minutes.

Table 3.4. Reagents for the assembly of four GB parts/superparts.

	pUPD2+KAT1 B3B4	**pUPD2+KAT1 B3B4B5**	**pUPD2+YFP B2**	**pUPD2+YFP B5**
40ng	KAT1-P1	KAT1-P1	YFP B2	YFP B5
40ng	KAT1-P2	KAT1-P2	-	-
40ng	KAT1-P3 B3B4	KAT1-P3 B3B4B5	-	-
75ng	pUPD2	pUPD2	pUPD2	pUPD2
3-4U	*BsmBI*	*BsmBI*	*BsmBI*	*BsmBI*
3U	T4 Ligase	T4 Ligase	T4 Ligase	T4 Ligase
1ul	Ligase Buffer 10X	Ligase Buffer 10X	Ligase Buffer 10X	Ligase Buffer 10X

Table 3.5. Reagents for the assembly of the four transcriptional units:* pα1*_YFP-KAT1,* pα1*_KAT1-YFP,* pα1*_KAT1 and* pα1*_YFP.

	pα1_YFP-KAT1	**pα1_KAT1-YFP**	**pα1_KAT1**	**pα1_YFP**
40ng	GB0552 (p35s for Nt fusion)	GB0030 (p35s)	GB0030 (p35s)	GB0030 (p35s)
40ng	pUPD2+YFP B2	pUPD2+KAT1 B3B4	-	-
40ng	pUPD2+KAT1 B3B4B5	pUPD2+YFP B5	pUPD2+KAT1 B3B4B5	GB0053 (pYFP B3B4B5)
40ng	GB0037 (pTnos)	GB0037 (pTnos)	GB0037 (pTnos)	GB0037 (pTnos)
75ng	pDGB3_alpha1	pDGB3_alpha1	pDGB3_alpha1	pDGB3_alpha1
3-4U	*BsaI*	*BsaI*	*BsaI*	*BsaI*
3U	T4 Ligase	T4 Ligase	T4 Ligase	T4 Ligase
1ul	Ligase Buffer 10X	Ligase Buffer 10X	Ligase Buffer 10X	Ligase Buffer 10X

3.4. Confocal microscopy

The fluorescence experiments were performed using an inverted Zeiss LSM780 confocal microscope (Zeiss, http://www.zeiss.com), using the argon laser with a Plan-Apochromat 40x/1.20 OIL DIC M27 objective and the ZEN 2001 software (Zeiss). YFP fluorescence was visualized by 488 nm excitation and emission was examined using a range of 500-555 nm. Chlorophyll fluorescence was visualized by 488 nm excitation and emission was examined using a range between 680-760 nm. Images were processed using Fiji software (processing package based on the ImageJ program).

4. Results

4.1. Domestication of the KAT1 sequence

The aim of the current project is to generate the reagents that can be used to test KAT1 protein-protein interactions with the 14 candidate proteins using BiFC. As explained in section 1.3 of the Introduction, a considerable number of constructions will be required for this purpose. In order to fulfill this task, GB 3.0 was the chosen cloning strategy. GB 3.0 is a modular system that allows for the assembly of different sequences (GB parts) to produce a transcriptional unit; and thus, it overcomes the first technical difficulty of the BiFC assay: the production of all the required constructions to perform the BiFC assay (Figure 1.5 shows the distinct combinations that must be considered to perform a BiFC assay).

Figure 4.1 summarizes how GB 3.0 grammar was applied to the full KAT1 sequence in order to adapt it for the purpose mentioned above. Figure 4.1 shows three distinct structures: the first one is a design for the expression of a single protein construct (Promoter+CDS+Terminator), the two following are designs to produce fusion proteins either in the N-terminus or the C-terminus. Figure 4.1, indicates the GB 3.0 grammar that each GB parts/superparts should have.

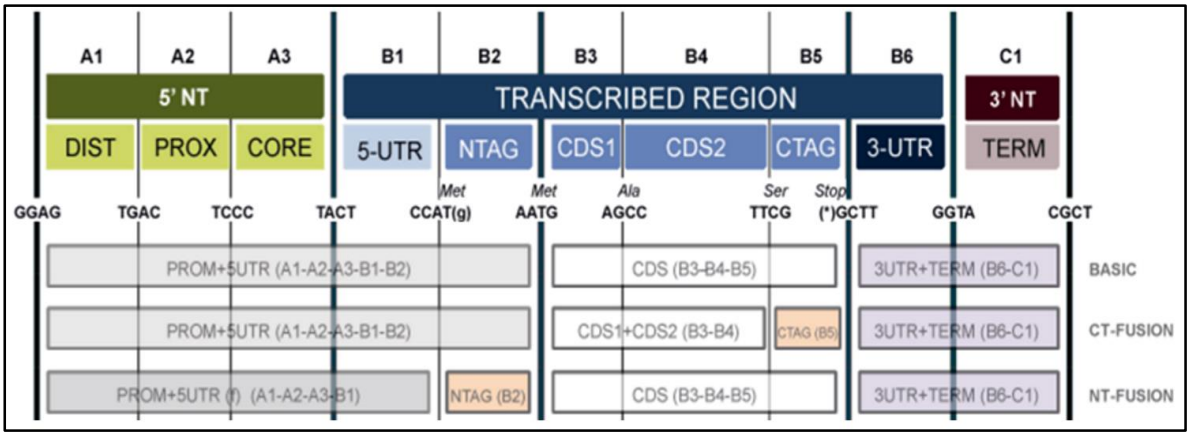

Figure 4.1. Transcriptional units design using GoldenBraid 3.0 grammar for a basic protein, N-terminal and C-terminal fusion proteins. *The grey box indicates the position of the promoter, the white box indicates the position of KAT1, the orange box indicates the position of the fusion protein and the purple box indicates the position of the Tnos, seen 17th April, 2016. Image modified from https://gbcloning.upv.es/do/multipartite/).*

The first step to initiate the GB experiment is referred as domestication. This domestication procedure consists of adapting the DNA building blocks to the GoldenBraid grammar. The design of the GB 3.0 adapted primers was performed using the resources offered by the web page: https://gbcloning.upv.es/tools/domestication/.

In order to perform the KAT1 domestication 7 primers were designed: 4 internal primers (to remove the internal *BsaI* and *BsmBI* restriction sites) and 3 external primers that included the desired GB 3.0 grammar (Figure 4.2). The KAT1 pieces were designed to allow the construction of fusion proteins either in the N-terminus or in the C-terminus. Following the GB 3.0 grammar shown in Figure 4.1, for a C-terminal KAT1 fusion a B3B4 fragment was constructed and the C-terminus fusion occupies the B5 position. For an N-terminal KAT1 fusion, a B3B4B5 fragment was constructed and the N-terminus fusion occupies the B2 position. So both KAT1 fragments will have in common the B3 overhang (5'-AATG-3') differing in the B4 (5'-TTCG-3') or B5 (5'-GCTT-3').

KAT1-P1 Fw	5' GCGCCGTCTCGCTCGAATGTCGATCTCTTGGACTCG 3'	Tm = 53.9°C
KAT1-P1 Rv	5' GCGCCGTCTCGGAAGACGCCATAACCTGAGC 3'	Tm = 54.7°C
KAT1-P2 Fw	5' GCGCCGTCTCGCTTCGGCGAGTTAGCTCGCT 3'	Tm = 57.8°C
KAT1-P2 Rv	5' GCGCCGTCTCGATGTCTCTTGTTGTTTCAAGCCC 3'	Tm = 54.3°C
KAT1-P3 Fw	5' GCGCCGTCTCGACATTGAACAATCTGCCAAAAGC 3'	Tm = 52.0°C
KAT1-P3 B3B4B5 Rv	5' GCGCCGTCTCGCTCAAAGCTCAATTTGATGAAAAATACAAATGATCAC 3'	Tm = 52.7°C
KAT1-P3 B3B4 Rv	5' GCGCCGTCTCGCTCACGAACCATTTGATGAAAAATACAAATGATCACC 3'	Tm = 51.4°C

Figure 4.2. Oligonucleotide sequences designed for KAT1 domestication as GoldenBraid 3.0 pieces. *Each sequence appears in two colors, blue letters indicate the sequence of the gene, and black letters indicate the added nucleotides for the GoldenBraid construction. The BsmBI recognition sites are highlighted in green, the overhang for the pUPD2 assembly is in red, and in purple the 4 letter grammar code to indicate the position of the fragment within the transcriptional unit. The red overhang will then reconstitute a BsaI recognition site. P1: patch 1; P2 patch 2; P3 patch 3.*

The domestication procedure for KAT1 consisted of 4 different PCR reactions: the first patch of 553 nucleotides, the second patch of 554 nucleotides, and two versions of the third patch: one for N-terminus fusion proteins and the other for C-terminus, 1014bp and 1013bp respectively. Each patch is generated in an independent PCR reaction in separate microtubes. The PCR conditions are indicated in Materials and Methods section 3.3.1 (PCR reagents Table 3.1 and conditions Table 3.2). Figure 4.3 shows the results of the corresponding PCR reactions and confirms that each reaction generated a single band of the expected size.

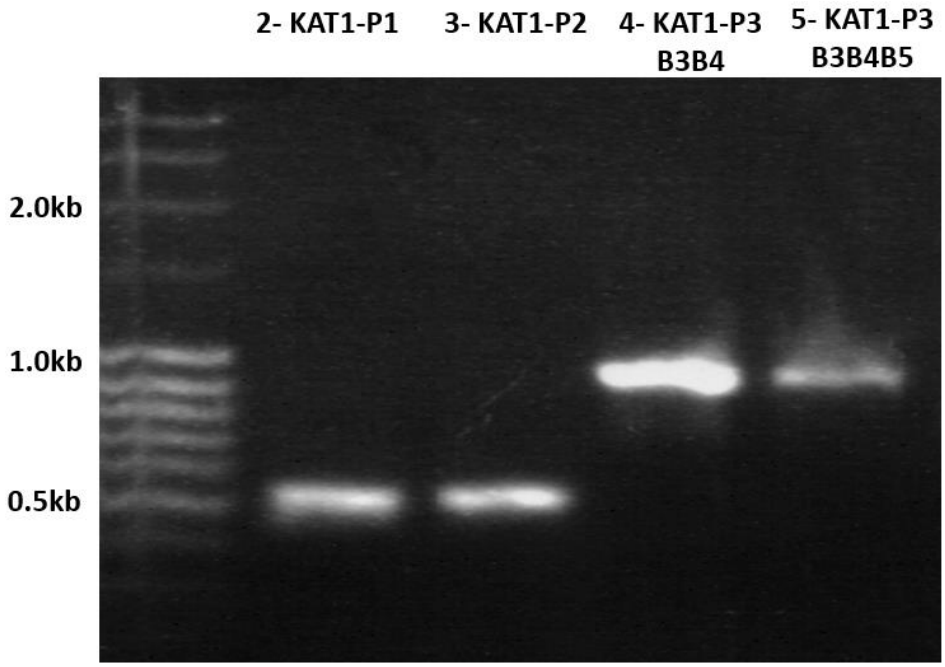

Figure 4.3. Visualization of the PCR products for KAT1 domestication. *The products of the indicated PCR reactions were separated on a 0.8% ethidium bromide-stained agarose gel. Lanes 2-5 correspond to the different KAT1 patches: KAT1-P1, KAT1-P2, KAT1-P3 B3B4 and KAT1-P3 B3B4B5. The molecular weight standard is shown in the first lane and the 2.0, 1.0 and 0.5kb markers are indicated on the left.*

After checking that the PCR products were correct, a digestion-ligation reaction was performed with the different patches to assemble the whole KAT1 B3B4 and KAT1 B3B4B5 fragments, and insert them into the domestication vector pUPD2, concluding the domestication procedure. The digestion-ligation reaction was performed as indicated in Table 3.4 of Materials and Methods section 3.3.2.

This digestion-ligation approach of the amplified products aims on one hand, to remove internal restriction sites in the genes of interest and on the other hand, the primers used in the PCR reactions include the required overhangs at the end of KAT1 sequences in order to define their position in the future transcriptional unit. The generation of each of the two GB parts is performed by two independent reactions, two different digestion-ligation reactions using the *BsmBI* restriction enzyme and introducing the pUPD2 domesticator plasmid.

The product of the digestion-ligation was used to transform *E. coli*, and 4 white colonies of each of the two constructs were analyzed by an EcoRI digestion (Figure 4.4).

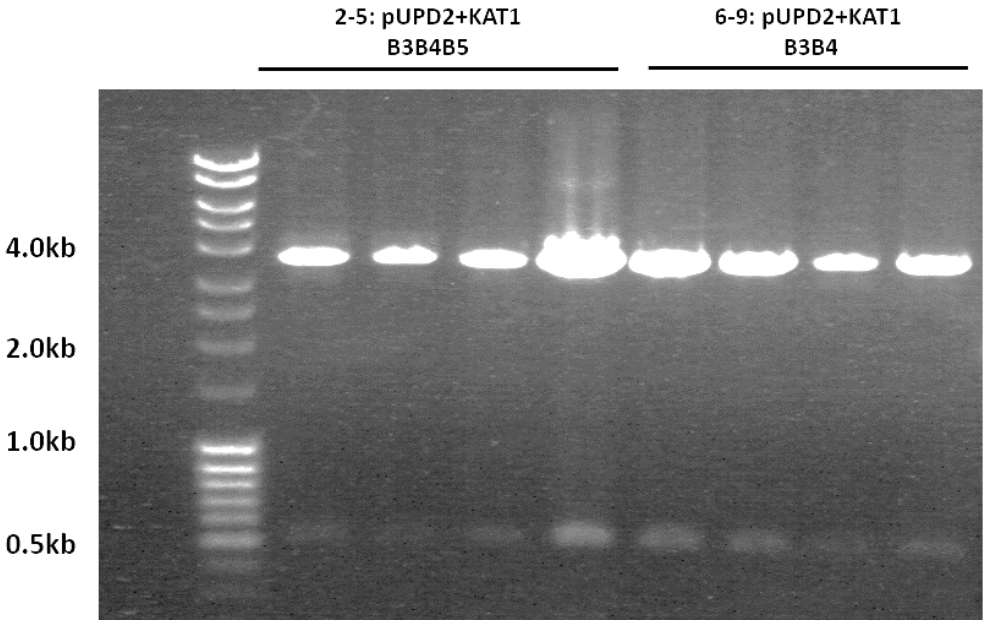

Figure 4.4. Visualization of the digestion pattern of DNA extracted from several colonies of the different KAT1 GB parts. *The digestion products were separated on a 0.8% ethidium bromide-stained agarose gel. 4 colonies of each construct were analyzed: lanes 2-5 correspond to pUPD2+KAT1 B3B4B5 and lanes 6-9 correspond to pUPD2+KAT1 B3B4. All of the analyzed plasmids were digested with EcoRI. The molecular weight standard is shown in the first lane and the 4.0, 2.0, 1.0 and 0.5kb markers are indicated on the left.*

Each of the clones analyzed presented digestion products of the expected size. All of the pUPD2+KAT1 clones presented the right pattern of bands: a band of almost 4kb and a lower band of 0.5kb.

Figure 4.5 summarizes the process for the domestication of KAT1 as a GB 3.0 part. The expected length of each fragment is indicated in the Figure as are the GoldenBraid codes used for assembly.

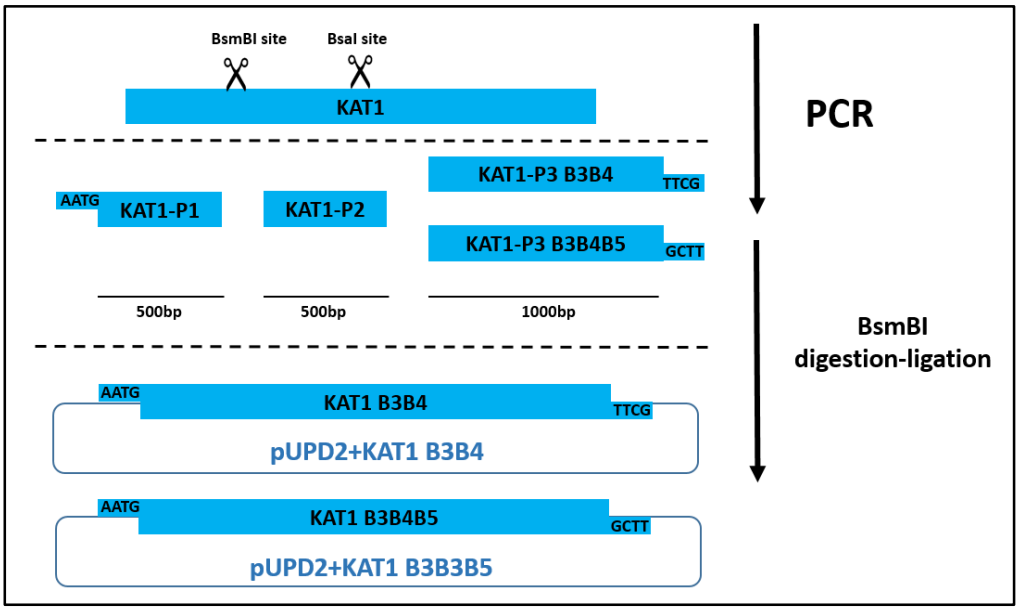

Figure 4.5. Schematic representation of the domestication process for KAT1. *Two steps were performed in the domestication: the PCR of each gene and the BsmBI digestion-ligation reaction to assemble the different parts into the domestication vector, pUPD2. The GoldenBraid grammar 3.0 is indicated as B followed by a number (i.e. B3B4). The different KAT1 patches are referred to as P1, P2, and P3.*

Each of the constructs was then confirmed by sequencing. An internal primer called KAT1-1831-F was used (described in the annex) to sequence these constructions. This primer anneals at the 3' end of the KAT1 gene and therefore the resulting sequence includes the B3B4 or B3B4B5 section to confirm the identity of each construct. The sequencing results were successful as shown in Figure 4.6.

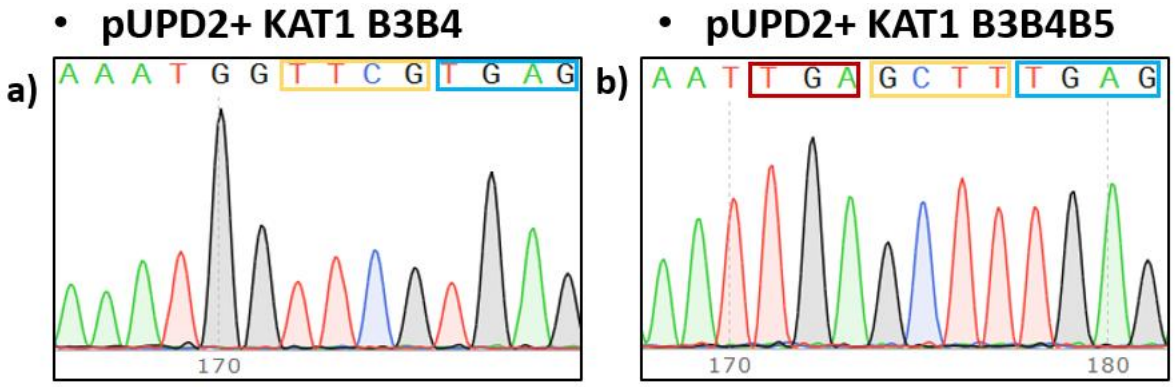

Figure 4.6. Chromatogram of the sequencing results for pUPD2+KAT1 B3B4 and pUPD2+KAT1 B3B4B5. *Sequencing results showing the 3' end of the KAT1 gene. The yellow box indicates the GoldenBraid grammar code, which is correct in all cases. The blue box indicates the overhang to assemble with the pUPD2 and the red boxes indicate the STOP codon. a) pUPD2+KAT1 B3B4 b) pUPD2+KAT1 B3B4B5.*

Figure 4.6 a) shows the two extra nucleotides (GG) added at the end of the KAT1 sequence sequence to maintain the reading frame in C-terminal constructs. On the other hand, KAT1 B3B4B5 did not require these extra nucleotides and contains a STOP codon, Figure 4.6 b).

The final products: pUPD2+KAT1 B3B4 and pUPD2+KAT1 B3B4B5; represent a solid design of the KAT1 sequence as GB 3.0 parts that can be implemented to produce different transcriptional units. These GB parts will be able to assemble with other protein fusions, such as YFN/YFC and produce the constructions required for the BiFC assay: YFN fused to either the N-terminus or C-terminus of KAT1 (YFN-KAT1 or KAT1-YFN), and YFC fused to either the N-terminus or C-terminus of KAT1 (YFC-KAT1 or KAT1-YFC). However, the fusion of YFN/YFC might alter the normal localization or accumulation of KAT1. If KAT1 localization were altered by the N-terminal or C-terminal fusion of YFN/YFC it would be recommended to eliminate this fusion combination from the BiFC analysis. So, prior to the BiFC assay, the construction of the yellow fluorescent protein fused to KAT1 either in the N-terminus or the C-terminus (YFP-KAT or KAT1-YFP) was designed.

The analysis of the fluorescent expression of these two fusion proteins, YFP-KAT1 and KAT1-YFP, will provide a valuable tool to functionally analyze the effect of an N-terminal or C-terminal fusion on KAT1 and therefore eliminate from the BiFC assay the combinations that may alter KAT1 localization and to confirm that all of the steps of the *A. tumefaciens*-mediated transient transformation of *N. benthamiana* function properly. These reagents can also be used to study different aspects of KAT1 trafficking. Therefore, this procedure will produce useful information and valuable tools for future applications.

4.2. YFP sequence design

As mentioned above, one aim of the current project was the construction of two KAT1 fusion proteins: the Yellow Fluorescent Protein (YFP) fused to the N-terminal end of the protein, YFP-KAT1, and the YFP fused to the C-terminal end of the protein, KAT1-YFP. With this aim, two YFP sequences had to be designed in order to be able to introduce them as an N-terminal or C-terminal fusions into the transcriptional unit. Moreover, a short linker had to be introduced between YFP and KAT1 to enable the flexibility of the fusion protein, and will facilitate the use of the same designed structure for the BiFC assay that will follow this work. Based on the amino acid sequences suggested by Kerppola and colleagues the peptide linker was: SAGTI (Hu and Kerppola, 2003). This linker takes into account the introduction of a short sequence that would facilitate the posterior design of the BiFC constructions and at the same time would provide a flexible peptide linker between the two proteins.

YFP had to be designed to occupy either a B2 (for N-terminal fusions) or a B5 (for C-terminal fusions) position, as indicated in Figure 4.1.

Linker-YFP B5 Fw	5′ GCGCCGTCTCGCTCGTTCGTCTGCAGGTACTATTATGGTGAGCAAGGGCGAGGA 3′	Tm = 61.4°C
Linker-YFP B5 Rv	5′ GCGCCGTCTCGCTCAAAGCTCAGCTCATGACTGACTTGTAGAGCTC 3′	Tm = 59.5°C
YFP-Linker B2 Fw	5′ GCGCCGTCTCGCTCGCCATGGTGAGCAAGGGCGAG 3′	Tm = 57.9°C
YFP-Linker B2 Rv	5′ GCGCCGTCTCGCTCACATTGAAATAGTACCTGCAGAGCTCATGACTGACTTGTAGAGCTC 3′	Tm = 57.0°C

Figure 4.7. Oligonucleotide sequences designed for YFP adaptation as GoldenBraid 3.0 pieces. *Each sequence appears in two colors, blue letters indicate the sequence of the gene, and black letters indicate the added nucleotides for the GoldenBraid construction. The BsmBI recognition sites are highlighted in green, the overhang for the pUPD2 assembly is in red, and in purple the 4 letter grammar code to indicate the position of the fragment within the transcription unit. The red overhang will then reconstitute a BsaI recognition site. The underlined sequence corresponds to the linker that will be between KAT1 and YFP in both fusion constructs.*

The expected lengths were 782bp for YFP B2, and 785bp for YFP B5. The PCR was conducted as indicated in Materials and Methods section 3.3.1 (PCR reagents Table 3.1 and PCR conditions Table 3.3). Figure 4.8 shows the results of the corresponding PCR reactions and confirms that each reaction generated a single band of the expected size.

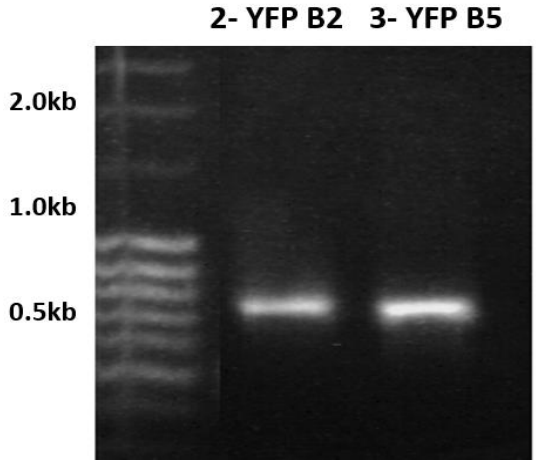

Figure 4.8. Visualization of the PCR products for YFP domestication. *The products of the indicated PCR reactions were separated on a 0.8% ethidium bromide-stained agarose gel. Lanes 2 and 3 correspond to full YFP B2 and YFP B5 sequences. The molecular weight standard is shown in the first lane and the 2.0, 1.0 and 0.5kb markers are indicated on the left.*

After checking that the PCR products were correct, a digestion-ligation reaction was performed to insert YFP B2 and YFP B5 into the domestication vector pUPD2. The digestion-ligation reaction was performed as indicated in Table 3.4 of Materials and Methods section 3.3.2. The generation of each of the two GB parts is performed by two independent different digestion-ligation reactions using the *BsmBI* restriction enzyme and introducing the pUPD2 domesticator plasmid.

The product of the digestion-ligation was used to transform *E. coli*, and 4 white colonies of each two constructs were analyzed by an *XhoI* digestion (Figure 4.9).

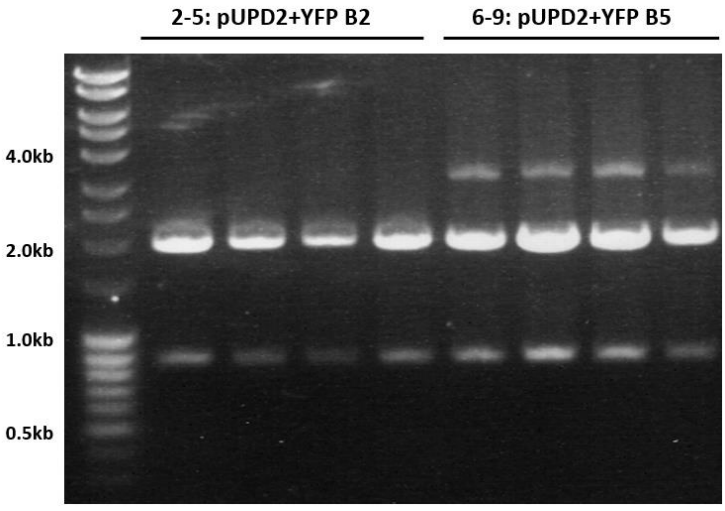

Figure 4.9. Visualization of the digestion pattern of DNA extracted from several colonies of the different YFP GB parts. *The digestion products were separated on a 0.8% ethidium bromide-stained agarose gel. 4 colonies*

of each construct were analyzed: lanes 2-5 correspond to pUPD2+YFP B2 and lanes 6-9 correspond to pUPD2+YFP B5. All of the analyzed plasmids were digested with XhoI. The molecular weight standard is shown in the first lane and the 4.0, 2.0, 1.0 and 0.5kb markers are indicated on the left.

For both pUPD2+YFP vectors, the same pattern was expected: a band of 2kb and a band of approximately 0.9kb. The pUPD2+YFP B5 clones presented an extra band around 3kb that was attributed to the undigested plasmid.

Each of the constructs was then confirmed by sequencing. In order to sequence the YFP constructs, the same forward primers used in the domestication was used: YFP-Linker B2 Fw and Linker-YFP B5 Fw. The sequencing results were successful as shown in Figure 4.10.

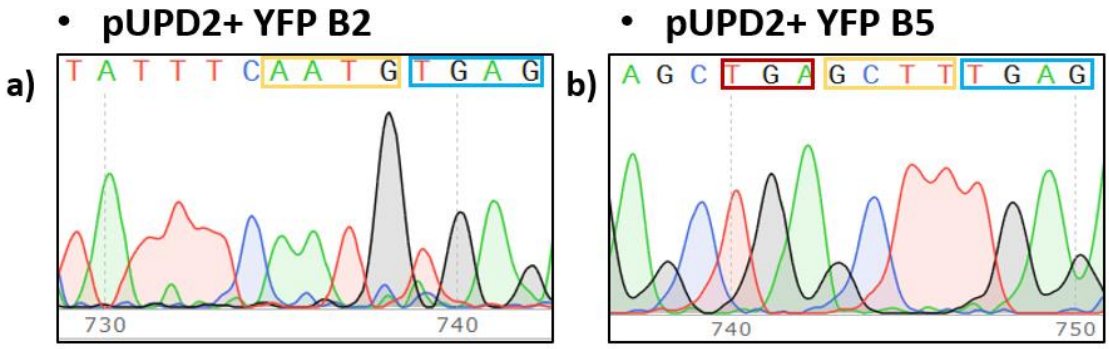

Figure 4.10. Chromatogram of the sequencing results for pUPD2+YFP B2 and pUPD2+YFP B5. *Sequencing results showing the 3' end of the YFP gene. The yellow box indicates the GoldenBraid grammar code, which is correct in all cases. The blue box indicates the overhang to assemble with the pUPD2 and the red boxes indicate the STOP codon. a) pUPD2+YFP B2 b) pUPD2+YFP B5.*

Figure 4.10 a) shows two extra nucleotides (TC) added at the end of the YFP sequence, after the linker, to maintain the reading frame in N-terminal constructs. On the other hand, YFP B5 did not require these extra nucleotides and contains a STOP codon, Figure 4.10 b).

The result was two GB 3.0 parts: pUPD2+YFP B2 and pUPD2+YFP B5. These GB 3.0 parts were then able to be assembled with the KAT1 GB 3.0 parts to produce YFP-KAT1 and KAT1-YFP constructions.

4.3. Assembly of the transcriptional units

At this point, the KAT1 sequence was designed as a modular piece that can be assembled to produce different transcriptional units required to perform a BiFC assay. However, it is a priority to minimize the complexity of the BiFC assay, if possible. Therefore, we were interested in testing the functionality of protein fusions at both the N- and C- terminus of KAT1. If either of these fusions disrupts KAT1 stability or trafficking it will be eliminated from the BiFC assay.

In order to perform this functional analysis, the structures shown Figure 4.1 were used to produce the GB parts to construct the N-terminal and C-terminal fusions, YFP-KAT1 and KAT1-YFP. In addition, the design of a basic transcriptional unit was used to construct the positive and negative controls: YFP and KAT1; respectively. So the four transcriptional units were: pα1_YFP (positive control), pα1_KAT1 (negative control), pα1_YFP-KAT1 (N-terminal fusion) and pα1_KAT1-YFP (C-terminal fusion). The digestion-ligation reaction for the assembly of these transcriptional units was performed as explained in Materials and Methods section 3.3.2 Table 3.5.

Figure 4.11 summarizes the process followed to construct the 4 desired transcriptional units by means of a digestion-ligation using the *BsaI* enzyme.

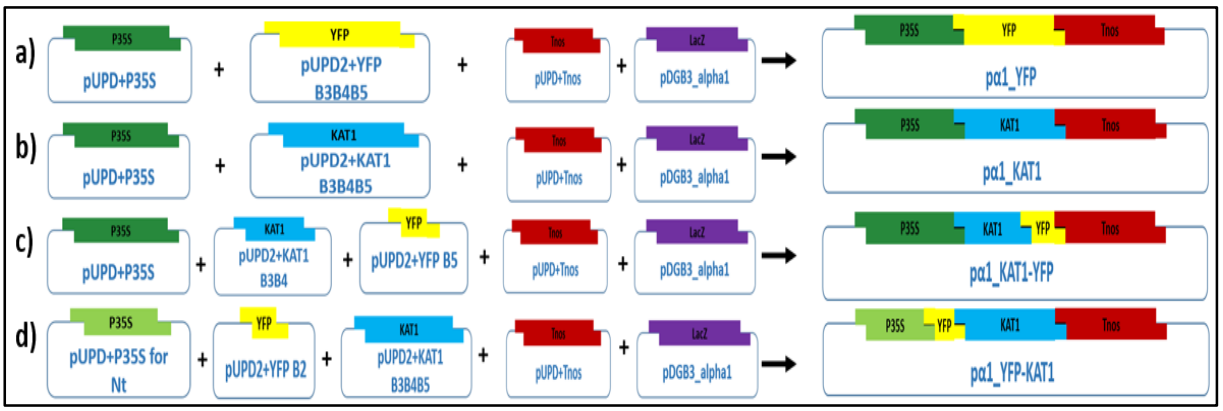

Figure 4.11. Diagram of the construction of the 4 transcriptional units. *The parts for the assembly of the positive control are depicted for each transcriptional unit: a) pα1_YFP; b) pα1_KAT1; c) pα1_KAT1-YFP; d) pα1_YFP-KAT1.*

Figure 4.12 shows the restriction analysis using an *EcoRI* digestion of plasmid DNA extracted from the selected colonies from the transformation with the digestion-ligation product to generate the pα1_YFP-KAT1 and pα1_KAT1 constructs. Three colonies of each construct were analyzed and two of each showed the correct restriction pattern.

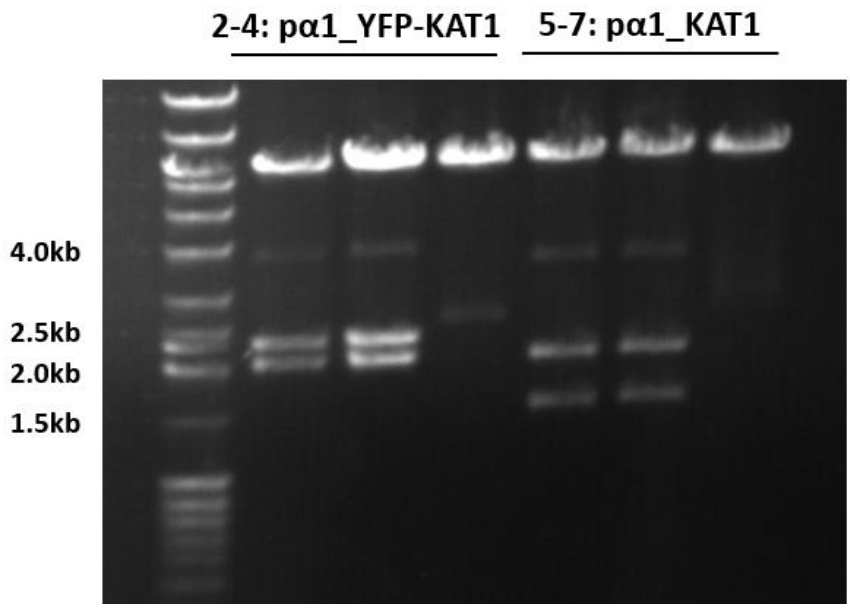

Figure 4.12. Visualization of the digestion pattern of DNA extracted from several colonies of pα1_YFP-KAT1 and pα1_KAT1. *The digestion products were separated on a 0.8% ethidium bromide-stained agarose gel. 3 colonies of each construct were analyzed: lanes 2-4 correspond to pα1_YFP-KAT1 and lanes 6-9 correspond to pα1_KAT1. All of the analyzed plasmids were digested with EcoRI. The molecular weight standard is shown in the first lane and the 4.0, 2.5, 2.0 and 1.5kb markers are indicated on the left.*

The construction pα1_YFP-KAT1 digested with *EcoRI* shows the following restriction pattern: 6.3kb, 2.3kb and 2.1kb. Lanes 2 and 3, in Figure 4.12, presented this restriction pattern. However, an additional band around 4kb was also observed. In order to generate a pure preparation without

this contaminating band, the DNA extracted from one of the colonies was used to retransform *E.coli*. The same occurred with the pα1_KAT1 construct which when digested with EcoRI, presenting the following restriction pattern: 6.3kb, 2.1kb and 1.5kb. Again, the restriction pattern shown in Figure 4.12 was correct for the clones assayed in lanes 5 and 6, but with an extra band at 4kb which was also attributed to co-transformation. The DNA from one of the colonies was used to retransform *E. coli*. The same process was applied for the other two constructions: pα1_KAT1-YFP and pα1_YFP; colonies were analyzed by *EcoRI* digestion and when the product was correct but with additional contaminating bands, they were re-transformed and re-purified. The pα1_KAT1-YFP construction had a restriction pattern of 6.3kb, 2.8kb and 1.5kb, while pα1_YFP had a restriction pattern of 6.3kb and 2.3kb. Figure 4.13 shows the final digestion analysis obtaining pure clones of all 4 constructions.

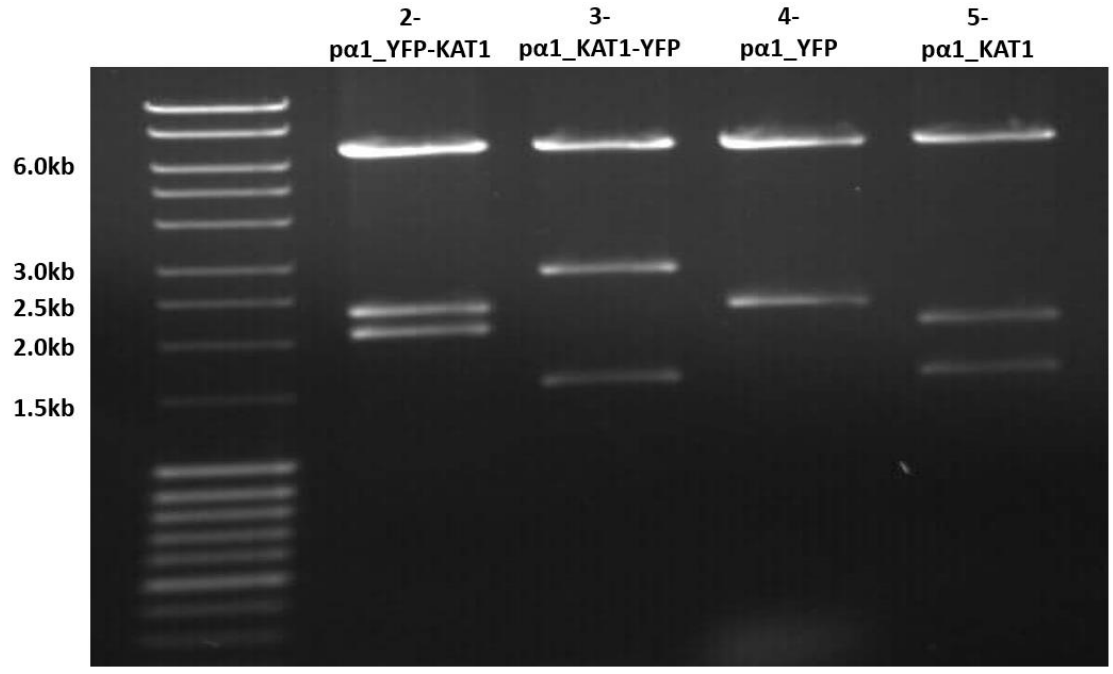

Figure 4.13. Visualization of the digestion pattern of DNA extracted from a colony of pα1_YFP-KAT1, pα1_KAT1-YFP, pα1_YFP and pα1_KAT1. *The digestion products were separated on a 0.8% ethidium bromide-stained agarose gel. 1 colony of each construct was analyzed. Lane 2: pα1_YFP-KAT1; lane 3: pα1_KAT1-YFP; lane 4: pα1_YFP; lane 5: pα1_KAT1. All of the analyzed plasmids were digested with EcoRI. The molecular weight standard is shown in the first lane and the 6.0, 3.0, 2.5, 2.0 and 1.5kb markers are indicated on the left.*

Each construct was then confirmed by sequencing.

4.4. Analysis of the expression and subcellular localization of the GoldenBraid contructs

Once the 4 constructs were correctly inserted into the pCambia vector (pDGB3_alpha1), the generated constructs were transiently transfected into *N. benthamiana* plants using *A. tumefaciens.* Areas around the infiltration sites were analyzed by confocal microscopy, using an excitation wavelength of 488nm and observing the YFP emission in the range from 500nm to 555nm (green channel). The generated images were also analyzed for the fluorescence emitted by the chlorophyll that was excited at 488 and its emission was analyzed from 680nm to 760nm (red channel), in order to locate the chloroplasts in the cell. Representative images obtained for the YFP (positive control), KAT1-YFP (C-terminal fusion protein) and KAT1 (negative control) are shown in Figure 4.14.

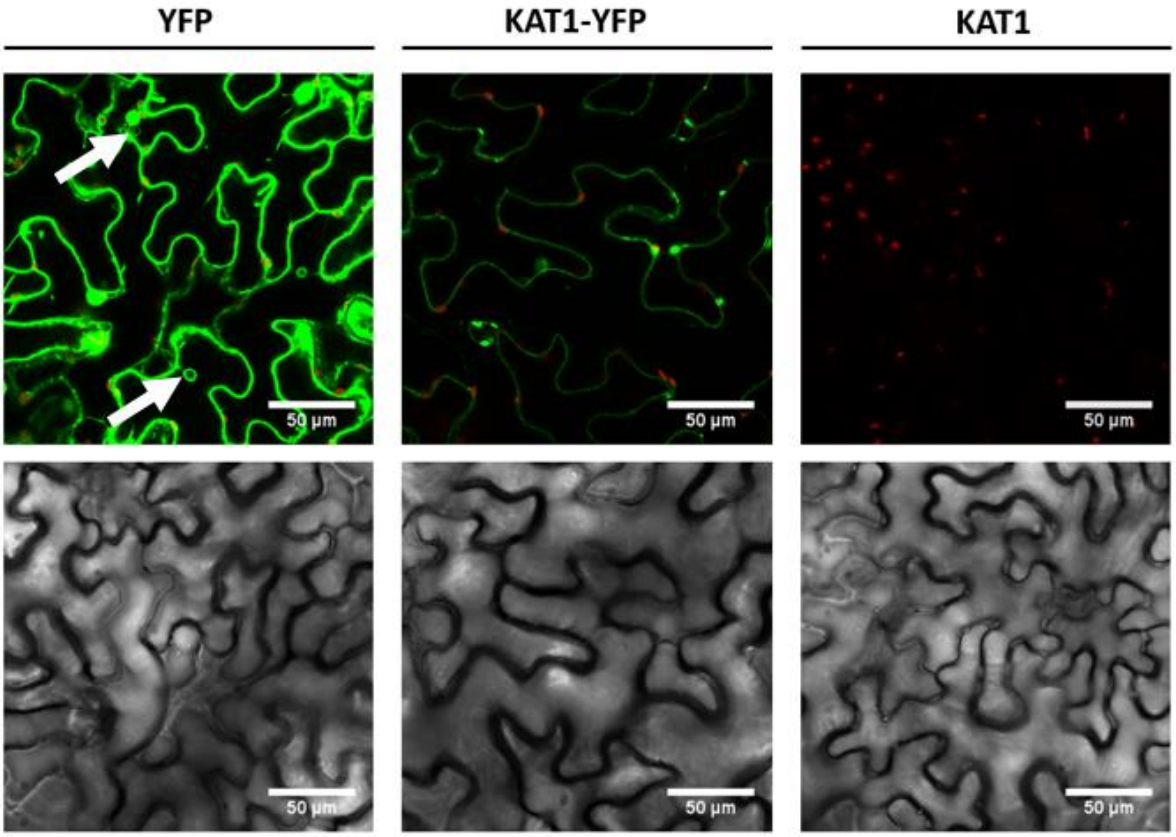

Figure 4.14. Confocal microscopy images of YFP, KAT1-YFP and KAT1. *Green channel: YFP fluorescence; red channel: chlorophyll fluorescence. The top three images correspond to the fluorescence images while the images in the bottom correspond to the transmitted light. Left column: pα1_YFP; middle column: pα1_KAT-YFP; and right column: pα1_KAT1. These images correspond to the samples analyzed 48h after infiltration.*

To generate the confocal microscopy images, the acquisition conditions of the positive and negative control samples were optimized. Briefly, the gain was set at a value that allowed the optimal observation of the YFP fluorescence and no background fluorescence for the KAT1 negative control. The KAT1-YFP and YFP-KAT1 samples were then analyzed using these conditions.

This preliminary experiment shows the fluorescence of YFP, KAT1-YFP and KAT1 at 48h after infiltration. We chose the C-terminal KAT1 fusion for this preliminary experiment based on reports in the literature of the successful observation of the C-terminal fusion of fluorescent proteins to KAT1 (Sutter *et al., 2006;* Sutter *et al.,* 2007). We observed, as expected, that YFP accumulates to much higher levels than the KAT1-YFP fusion protein. We also confirm the well-described cytoplasmic localization of free YFP, while the fluorescence pattern observed for KAT1-YFP is consistent with its localization in the plasma membrane. The cytosolic localization of free YFP is based on the observation of circular patterns, which are due to the presence of cytoplasmic organelles where free YFP is excluded (white arrows). This pattern is characteristic of cytosolic localization. In the case of KAT1-YFP, the fluorescence signal is observed only at the cell surface and no evidence of organelle exclusion is observed. This pattern was also confirmed in the experiments described below.

We next carried out a time course analysis of the expression of the YFP and KAT1 constructs fused to both the N- and C-terminus, analyzing the fluorescence at 24, 48 and 72 hours. Each of the constructs was transformed into Agrobacterium and transient transfections of *N. benthamiana* were carried out as described in Materials and Methods sections 3.2.3 and 3.2.4. Representative

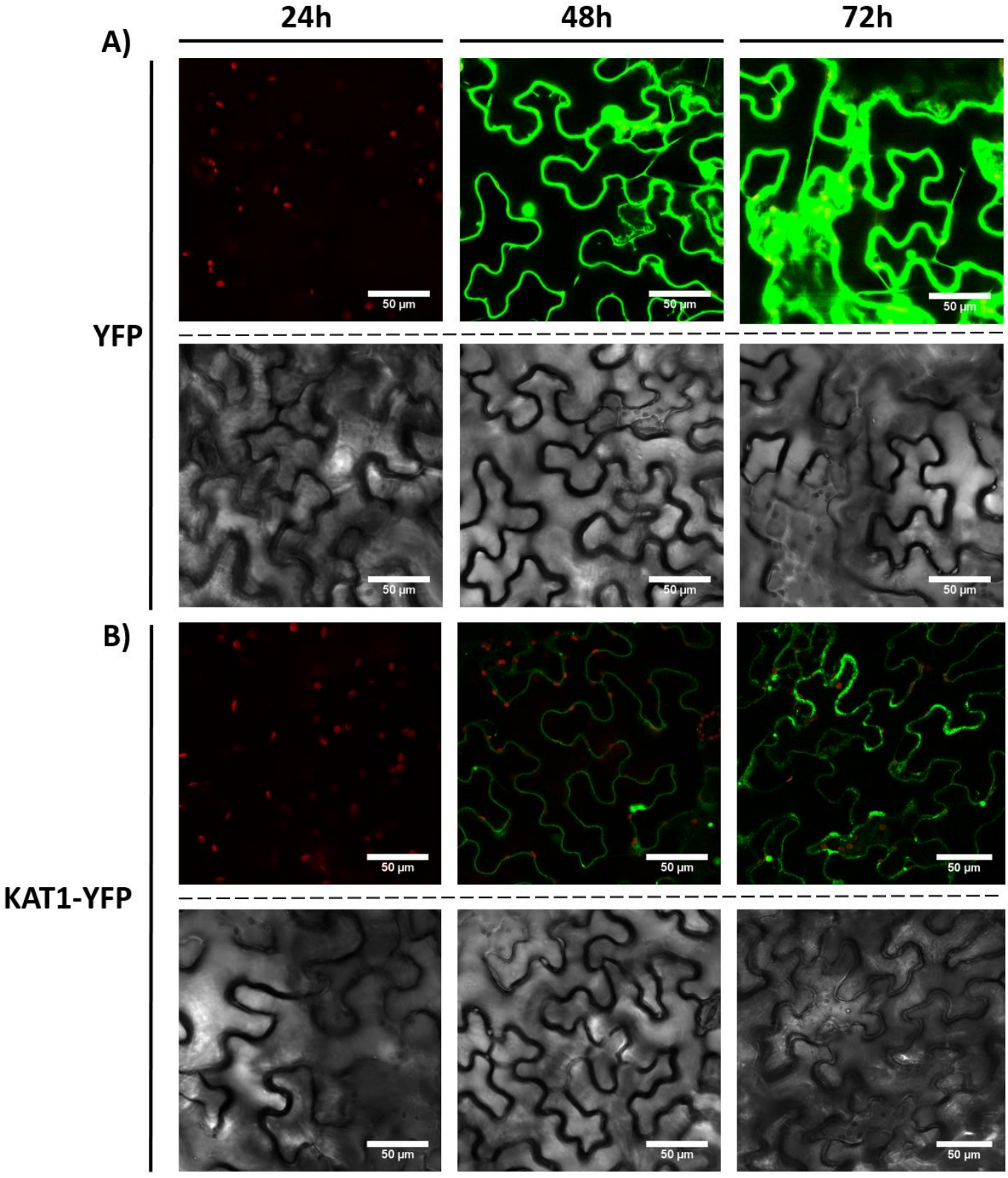

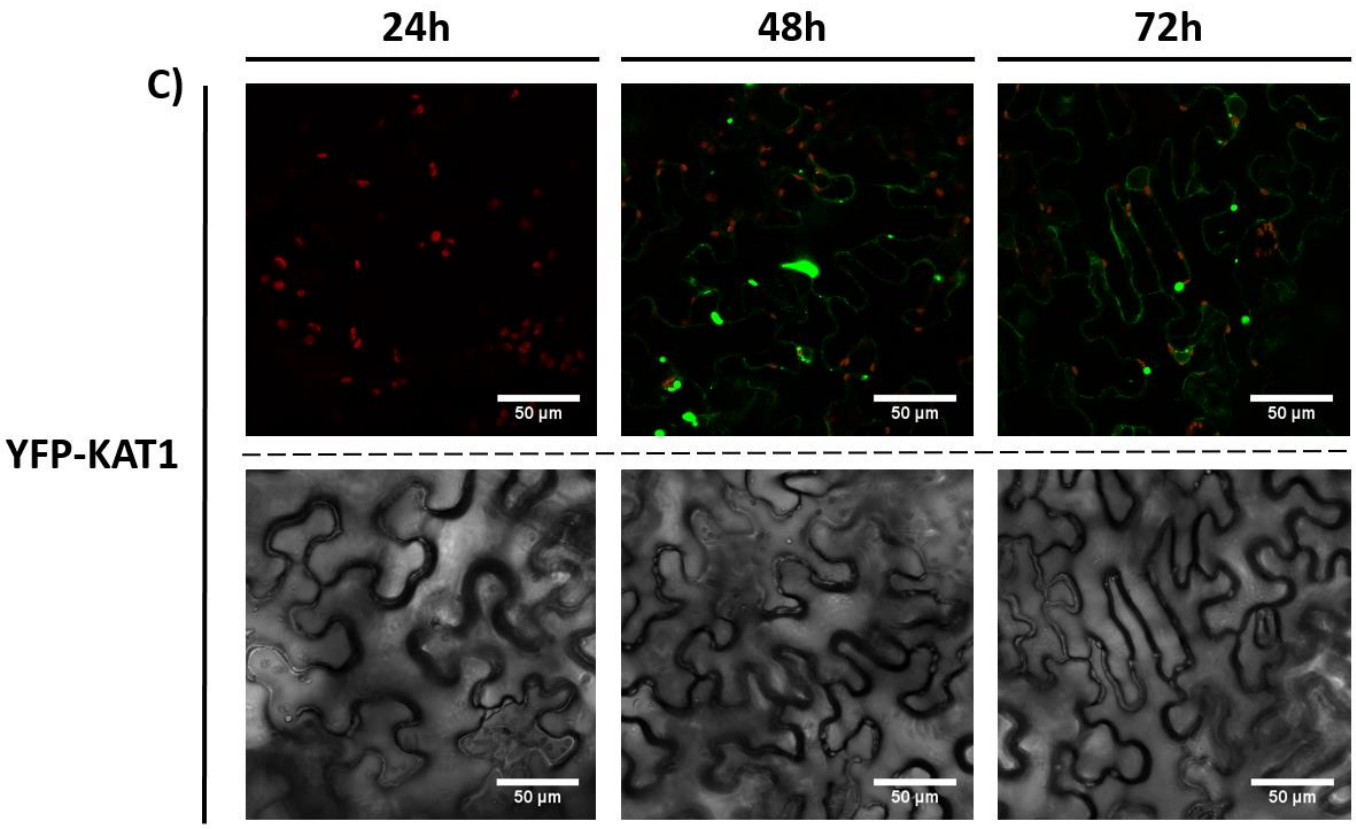

Figure 4.15. Time course of fluorescent protein expression. *Representative confocal microscopy images of the expression of the indicated constructs (pα1_YFP, pα1_KAT1-YFP and pα1_YFP-KAT1) were taken at 24, 48 and 72 hours after infiltration are shown. Green channel: YFP fluorescence; red channel: chlorophyll fluorescence. For A), B) and C) the three images in the top correspond to the fluorescence analysis and the three bottom images correspond to the transmitted light.*

The fluorescence microscopy analysis were done in three leaf sections for each construct and condition and the entire experiment, starting from the *Agrobacterium* infiltration, was repeated twice. Essentially identical results were observed in all samples.

With respect to time, all three constructions (YFP, KAT1-YFP and YFP-KAT1) showed an important increase from 24 to 48h, since no fluorescence was detected at 24h, while at 48h consistently high-level expression was observed for YFP and for KAT1-YFP to a lower degree. The YFP-KAT1 fusion protein showed a lower expression than KAT-YFP. The highest level of expression for all of the proteins was observed at 72h, where YFP reached a remarkable level of fluorescence. Regarding the cellular location, as mentioned above, YFP was expressed in the cytoplasm. The white arrows in Figures 4.14 and 4.16 indicate the fluorescent areas where the cytoplasmic location of YFP is observed based on its exclusion from organelles, including the chloroplasts. In the case of KAT1-YFP, the fusion protein appeared at a subcellular localization that is consistent with the cell membrane, as would be expected. A fluorescence signal is also observed in large punctuate regions, which are still undefined, but may correspond to ER, Golgi or intracellular vesicles. Consistent with the hypothesis is the fact that less of these punctuate structures are observed at 72h, maybe

suggesting that they represent intermediate localizations of KAT1 prior to plasma membrane delivery. Further co-localization experiments are required to unequivocally confirm this hypothesis. In the case of the YFP-KAT1 fusion protein, the majority of the signal is observed in punctuate structures even at 72h post-infiltration, with a small percentage possibly arriving to the plasma membrane. These data suggest that the N-terminal fusion of YFP to the KAT1 coding sequence may impede its efficient delivery to the cell surface. This result suggests that this fusion protein is not properly localized and this information is extremely helpful for the design of the subsequent BiFC experiments.

We further analyzed the subcellular localization of these proteins by recording images through a series of planes and generating 3D images of the subcellular distribution. Figure 4.16 shows a 2D reconstruction of representative 3D Z-stacks.

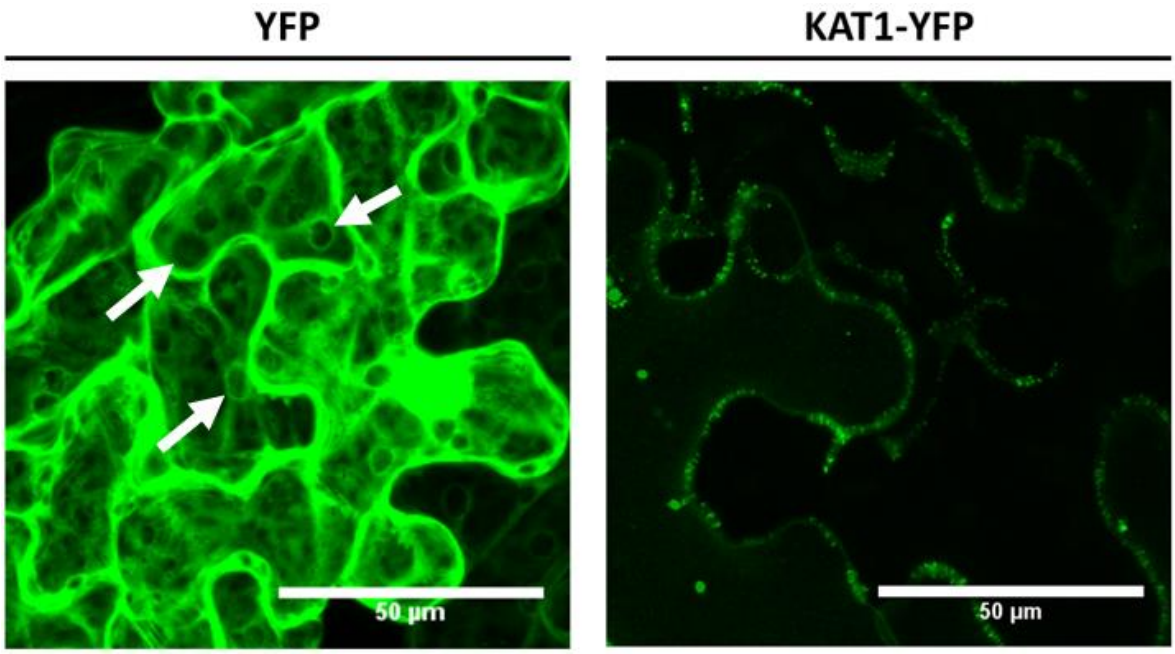

Figure 4.16. Confocal fluorescence microscopy analysis of YFP and KAT1-YFP. *Left: YFP; right: KAT1-YFP. Both images are obtained from a stack image i.e. a three dimensional image that has been converted to a 2D image fusing the Z-projection using the standard deviation in this Z plane. Green channel visualization. Both images correspond to the expression of the fusion proteins at 72 hours.*

The fusion of the Z-projection to transform a 3D image into a 2D image using the standard deviation clarifies the differences between the expression of YFP and KAT1-YFP (Figure 4.16). KAT1-YFP appears to accumulate unevenly at the cell membrane whereas YFP appears to accumulate in the cytoplasm (white arrows indicating the characteristic circular pattern). Similar results have been reported in the literature (Sutter *et al.,* 2006; Sutter *et al.,* 2007) and these structures observed for KAT1-YFP may represent lipid rafts, as will be discussed below.

5. Discussion

5.1. GoldenBraid 3.0 cloning system proved to be useful for the development of BiFC reagents

The modular nature of GB 3.0 ratified this cloning system as a suitable tool for the development of the BiFC assays. KAT1 was adapted as GB parts (pUPD2+KAT1 B3B4 and pUPD2+KAT1 B3B4B5) and these were used to produce N-terminal and C-terminal fusion proteins. This fact indicates that GB cloning can be used for the production of the complete set of fusion proteins to perform the BiFC assays and it could be applied to the 14 candidates to adapt them as KAT1 was adapted to the GB 3.0 system.

It must be taken into consideration the utility of binary vectors for the development of a BiFC assay (Citovsky *et al.,* 2006). The assembly of the BiFC expression cassettes (transcriptional units) into a single multigenic construct that is introduced into *A. tumefaciens* guarantees the equal expression of the desired proteins in the plant which would be crucial for the development of a BiFC. Therefore, this would reduce the likelihood of false negatives. GB, with its pCambia vector adapted to α and Ω levels covered this necessity and multigenic constructs will be able to be developed.

5.2. The transient expression of KAT1 in *Nicotiana benthamiana* was successful

Two KAT1 fusion proteins with the Yellow Fluorescent Protein (YFP) were constructed. An N-terminal and C-terminal fusion protein: YFP-KAT1 and KAT1-YFP. These two fusion proteins helped on one hand, to determine whether KAT1 constructions were able to be expressed in *N. benthamiana* using the GB cloning system, and on the other hand, to perform a functional analysis of the effect of an N-terminal and a C-terminal fusion. In addition, a YFP construct and a KAT1 construct were generated as positive and negative controls, respectively.

Among the four constructs that were generated, YFP, KAT1-YFP and YFP-KAT1 were observed to be expressed in *N. benthamiana* 48h after agroinfiltration, whereas the negative control KAT1 did not show any fluorescence. YFP presented a cytoplasmic localization in the cell, on the contrary KAT1-YFP and YFP-KAT1 were observed in punctuate structure and at the cell membrane (the expression of these proteins is discussed below in section 5.3).

The three fluorescent proteins (YFP, KAT1-YFP and YFP-KAT1) showed the same time course of accumulation: 24h after the agroinfiltration no fluorescence was detected, at 48h the three fluorescent proteins could be visualized, and finally, at 72h the highest level of expression was observed. These results indicate that the designed protocol allowed for the construction and expression of fusion proteins in *N. benthamiana* and that 72 hours after the agroinfliltration resulted in optimal visualization of the expression.

The different level of expression between YFP and the KAT1 fusion proteins (KAT1-YFP and YFP-KAT1) is explained because of the YFP properties. YFP is a highly stable protein of 27kDa which is not toxic for the cells. However, the stability of the potassium channel fusion constructs (KAT1-YFP and YFP-KAT1) might not be the same as YFP, resulting in a lower concentration of protein and thus a lower level of fluorescence. In addition, YFP is synthesized by cytosolic ribosomes while YFP-KAT1 and KAT1-YFP suffer a more complex process of synthesis end export that may reduce the efficiency of its expression.

The results obtained indicate that the designed GB parts were correctly assembled into the 4 transcriptional units (pα1_KAT1, pα1_YFP, pα1_KAT1-YFP and pα1_YFP-KAT1). These transcriptional units were controlled by the 35S promoter and terminator nos that proved to achieve a detectable level of expression. This suggests that the same protocol can be applied to analyze KAT1 protein-protein interactions with the 14 candidates using BiFC.

5.3. Differential expression and subcellular accumulation of KAT1-YFP and YFP-KAT1 in *Nicotiana benthamiana*

Prior to the BiFC assay, the expression of YFP-KAT1 and KAT1-YFP fusion proteins was carried out. This was performed not only to test the GB cloning system for the expression of KAT1 in *N. benthamiana*, but also to perform a functional analysis of the effect of an N-terminal and a C-terminal fusion of KAT1. The construction of a fusion protein may alter the normal localization of the protein, so this preliminary experiment was crucial in order to establish a working protocol for the future BiFC assay.

Previous studies have proven that the localization of proteins might be affected by the production of a fluorescent construct. These studies reported that C-terminal tagging with a fluorescent protein resulted in a lower effect over protein expression and localization than N-terminal tagging which resulted in a lower expression efficiency and mislocalization (Wiemann et al., 2003; Palmer and Freeman, 2004).

To analyze the effect of N-terminal or C-terminal protein tagging, two aspects must be taken into consideration: protein folding and signal peptides. The expression of proteins starts in the cytosolic ribosomes, starting their synthesis with the N-terminus. Chaperones prevent the amino acid emerging tail from folding until a whole domain has emerged. If the protein sequence is tagged with a fluorescent protein at the N-terminal end, this will be the first to fold and will possibly disrupt the normal folding and thus, the correct localization of the protein. On the contrary, C-terminal tagging is not predicted to disturb the natural order of protein folding and the protein could reach its native structure. Non-cytoplasmic proteins are exported to their corresponding locations by signal peptides which are usually located at the N-terminus of proteins. These signal peptides have been reported to be masked by the construction of fusion proteins in the N-terminal end of the protein (Wiemann *et al.,* 2003). This masking of signal peptides has an important effect on mitochondrial or plasma membrane proteins. However, it is important to mention that some proteins present signal peptides at the C-terminal end and C-terminal tagging could also mask the localization signal.

In our experiments, the KAT1-YFP and YFP-KAT1 fusion proteins were observed to have different subcellular localization patterns. At 48 after the agroinfiltration, both proteins were detectable in large punctate structures and at the cell surface. However, the C-terminal construction, KAT1-YFP resulted in a clearly higher level of expression as compared to the N-terminal construct. Moreover, at 72h post-infiltration the majority of the C-terminal fusion protein was localized to the plasma membrane, whereas the N-terminal fusion remained mostly within the punctate structures.

These facts lead to two plausible hypotheses: the N-terminal fusion could have altered the process by which the protein properly folds, or the presence of the N-terminal fusion prevents the

signal peptide from being recognized even though the protein keeps its native structure. However, these two hypotheses are not independent.

KAT1 is a membrane protein, and as described it presents 6 transmembrane segments, this means that as the protein is synthesized these segments are integrated in the cell membranes in the ER (Endoplasmic reticulum). This integration in the ER membrane as the synthesis occurs contributes to the protein folding. As a membrane protein, if KAT1 is not transported to the ER it would not adopt its native structure. This situation would connect the two hypotheses, being one the cause of the other, as the signal peptide may not be recognized due to steric hindrance and thus the protein is misfolded.

KAT1 has a well characterized structure with 6 transmembrane segments. It is known that the first transmembrane segment, TM1 contains a type II signal-anchor function, and this kind of signal peptide participates in the integration of TM segment in the membrane. The TM2 contains a stop-transfer signal. These two transmembrane segments, TM1 and TM2, have proven to integrate by themselves in the membrane while TM3 and TM4 failed to do so. However, TM3 and TM4 are likely to be post-translationally integrated in the membrane when a still uncharacterized specific interaction occurs between them. TM5 and TM6 presented the ability to integrate in the membrane, like TM1 and TM2 (Sato *et al.,* 2002). This phenomenon could explain the obtained results presented in Figure 4.15. The YFP fusion to the N-terminal end of KAT1 could alter the recognition of the first signal-anchor peptide in TM1 so that KAT1 would not be correctly translocated to the plasma membrane. However, TM5 and TM6 still preserve the signal-anchor and stop-transfer functions, and TM3 and TM4 could specifically interact and be integrated, so that it is likely that YFP-KAT1 still integrates in the ER membrane and arrives to the plasma membrane. Nevertheless, the likelihood of YFP-KAT1 being properly folded and translocated to the ER membrane is lower than in the case of KAT1-YFP. This phenomenon could explain why YFP-KAT1 is still able to reach the membrane, but to a considerably lower degree.

Regarding KAT1-YFP expression, Figure 4.16 reveals that the C-terminal fusion of KAT1 is perfectly able to reach the plasma membrane. These results have been previously reported (Sutter *et al,* 2006; Sutter *et al.,* 2007). This fusion shows that KAT1-YFP is not evenly distributed along the membrane (Figure 4.16). It has been proposed that this uneven distribution may be the result of the integration of the channel into lipid rafts. Cell membranes contain different lipid species, and lipid-lipid immiscibility gives rise to heterogeneities, termed lipid rafts. These rafts are ordered domains that are more tightly packed than the surrounding with a higher resistance degree to detergents. Some proteins are preferentially found in ordered raft domains. The KAT1 K^+ channel has been associated with moderately detergent-resistant fractions (Sutter *et al.,* 2006) and the detected uneven distribution of KAT1-YFP at the plasma membrane may corroborate the association of KAT1 with lipid rafts (Figure 4.16).

An interesting fact in concordance with the results of Sutter *et al.* (2006) is that the localization of KAT1 appears to be predominantly in the cell membrane. However, a small number of punctate structures are still observed within the cell at 72 hours (Figure 4.16). The fact that the frequency with which these structures are observed inversely correlates with the increase of fluorescence observed at the plasma membrane suggests that these puncta might represent the KAT1-YFP protein in subcellular compartments involved in protein processing and/or trafficking.

However, further experiments using co-localization of organelle markers would be required to definitively prove this hypothesis.

For example, the combination of YFP/RFP (Yellow Fluorescent Protein and Red Fluorescent Protein) has proved to be adequate for co-localization studies, even for BiFC, with the combination of YFN and YFC with the RFP (Citovsky *et al.,* 2006). To identify if these punctate structures are in the ER, an N-terminal calreticulin peptide signal (Fliegel *et al.,* 1989) and a C-terminal ER-retention sequence KDEL (Munro and Pelham, 1987) with the RFP could be used. And to determine if these punctate structures are in the Golgi apparatus, an N-terminal fusion of the α–2,6-sialyltransferase transmembrane segment (Munro, 1991) with RFP could be used. If these structures do not co-localize with either the ER or Golgi, we propose the use of Brefeldin A and Latrunculin A treatments. Brefeldin A is used to inhibit the transport of vesicles from the ER to Golgi (Klausner *et al.,* 1992) and Latrunculin A inhibits actin polymerization (Yarmola *et al.,* 2000). Therefore, Brefeldin A could be used to assess the influence of ER to Golgi inhibition on KAT1 distribution and Latrunculin A could be used to determine whether the punctate structures below the plasma membrane disappear, so that they would be identified as endosomal vesicles.

In conclusion, the KAT1-YFP fusion protein showed the expected efficiency and presented the correct localization of KAT1. The low efficiency in the expression of the YFP-KAT1 fusion protein leads to the conclusion that either the signal peptide is not perfectly recognized or the proteins is misfolded; for the BiFC assay, this would be translated into either the protein is not going to reach an expression to produce a level of fluorescence to detect the interaction (the whole fluorescent protein would not be reconstituted), or the protein is misfolded, so it could aggregate and produce non-specific interactions impeding proper analysis. For these reasons, the N-terminal fusions will be eliminated from the BiFC assay, so that only two fusion constructs will have to be designed to perform the BiFC assay with KAT1: KAT1-YFN and KAT1-YFC.

6. Conclusions

1. KAT1 was successfully domesticated and integrated as a GoldenBraid part. This allowed for the production of different KAT1 constructions that were expressed in *Nicotiana benthamiana.* Therefore, a working protocol to perform the BiFC assay has been established.
2. The expression of the KAT1-YFP and YFP-KAT1 fusion proteins revealed a different expression among these two fusion constructs. The N-terminal fusion with KAT1 resulted in a lower level of expression and a suboptimal localization of this fusion protein, as compared to the C-terminal fusion.
3. The N-terminal fusions with KAT1 will be discarded from the BiFC assays. The complexity of the BiFC assay will be reduced, as only two KAT1 C-terminal fusions will be generated to perform the protein-protein interaction analysis: KAT1-YFN and KAT1-YFC.

7. References

Acharya, B. R., Jeon, B. W., Zhang, W., & Assmann, S. M. (2013). Open Stomata 1 (OST1) is limiting in abscisic acid responses of Arabidopsis guard cells. New Phytologist, 200(4), 1049-1063.

Anderson, J. A., Huprikar, S. S., Kochian, L. V., Lucas, W. J., & Gaber, R. F. (1992). Functional expression of a probable Arabidopsis thaliana potassium channel in Saccharomyces cerevisiae. Proceedings of the National Academy of Sciences, 89(9), 3736-3740.

Anschütz, U., Becker, D., & Shabala, S. (2014). Going beyond nutrition: Regulation of potassium homoeostasis as a common denominator of plant adaptive responses to environment. Journal of Plant Physiology, 171(9), 670–687.

Arai, R., Ueda, H., Kitayama, A., Kamiya, N., & Nagamune, T. (2001). Design of the linkers which effectively separate domains of a bifunctional fusion protein. Protein engineering, 14(8), 529-532.

Assmann SM, Wang XQ. From milliseconds to millions of years: guard cells andenvironmental responses. Curr Opin Plant Biol 2001;4:421–8.

Bracha-Drori, K., Shichrur, K., Katz, A., Oliva, M., Angelovici, R., Yalovsky, S., & Ohad, N. (2004). Detection of protein–protein interactions in plants using bimolecular fluorescence complementation. The Plant Journal, 40(3), 419-427.

Citovsky, V., Lee, L. Y., Vyas, S., Glick, E., Chen, M. H., Vainstein, A., ... & Tzfira, T. (2006). Subcellular localization of interacting proteins by bimolecular fluorescence complementation in planta. Journal of molecular biology, 362(5), 1120-1131.

Clough, S. J., & Bent, A. F. (1998). Floral dip: a simplified method forAgrobacterium-mediated transformation ofArabidopsis thaliana. The plant journal, 16(6), 735-743.

Corratgé-Faillie, C., Jabnoune, M., Zimmermann, S., Véry, A.A., Fizames, C., and Sentenac, H. (2010). Potassium and sodium transport in non-animal cells: the Trk/Ktr/HKT transporter family. Cell Mol Life Sci 67, 2511-2532.

de Virgilio, M., Kiosses, W. B., & Shattil, S. J. (2004). Proximal, selective, and dynamic interactions between integrin αIIbβ3 and protein tyrosine kinases in living cells. The Journal of cell biology, 165(3), 305-311.

Fliegel, L., Burns, K., MacLennan, D. H., Reithmeier, R. A., & Michalak, M. (1989). Molecular cloning of the high affinity calcium-binding protein (calreticulin) of skeletal muscle sarcoplasmic reticulum. Journal of Biological Chemistry, 264(36), 21522-21528.

Gierth, M., Mäser, P., and Schroeder, J.I. (2005). The potassium transporter AtHAK5 functions in K(+) deprivation-induced high-affinity K(+) uptake and AKT1 K(+) channel contribution to K(+) uptake kinetics in Arabidopsis roots. Plant Physiol 137, 1105-1114.

González, W., Riedelsberger, J., Morales-Navarro, S. E., Caballero, J., Alzate-Morales, J. H., González-Nilo, F. D., & Dreyer, I. (2012). The pH sensor of the plant K+-uptake channel KAT1 is built from a sensory cloud rather than from single key amino acids. Biochemical Journal, 442(1), 57-63.

Holsters, M., de Waele, D., Depicker, a., Messens, E., van Montagu, M., & Schell, J. (1978). Transfection and transformation of Agrobacterium tumefaciens. MGG Molecular & General Genetics, 163(2), 181–187.

Horstman, A., Tonaco, I. A. N., Boutilier, K., & Immink, R. G. (2014). A cautionary note on the use of split-YFP/BiFC in plant protein-protein interaction studies. International journal of molecular sciences, 15(6), 9628-9643.

Hoshi, T. (1995). Regulation of voltage dependence of the KAT1 channel by intracellular factors. The Journal of general physiology, 105(3), 309-328.

Hosy E, Duby G, Véry AA, Costa A, Sentenac H, Thibaud JB (2003) A procedure for localization and electrophysiological characterization of ion channels heterologously expressed in a plant context. Plant Methods 19:1-14.

Hu, C. D., & Kerppola, T. K. (2003). Simultaneous visualization of multiple protein interactions in living cells using multicolor fluorescence complementation analysis. Nature biotechnology, 21(5), 539-545.

Hynes, T. R., Mervine, S. M., Yost, E. A., Sabo, J. L., & Berlot, C. H. (2004). Live cell imaging of Gs and the β2-adrenergic receptor demonstrates that both αs and β1γ7 internalize upon stimulation and exhibit similar trafficking patterns that differ from that of the β2-adrenergic receptor. Journal of Biological Chemistry, 279(42), 44101-44112.

Jeanguenin, L., Alcon, C., Duby, G., Boeglin, M., Chérel, I., Gaillard, I., ... & Véry, A. A. (2011). AtKC1 is a general modulator of Arabidopsis inward Shaker channel activity. The Plant Journal, 67(4), 570-582.

Jiang, Y., Lee, A., Chen, J., Ruta, V., Cadene, M., Chait, B.T., and MacKinnon, R. (2003). X-ray structure of a voltage-dependent K+ channel. Nature 423, 33-41.

Kerppola, T. K. (2006). Visualization of molecular interactions by fluorescence complementation. Nature reviews Molecular cell biology, 7(6), 449-456.

Klausner, R. D., Donaldson, J. G., & Lippincott-Schwartz, J. (1992). Brefeldin A: insights into the control of membrane traffic and organelle structure. J. Cell Biol, 116(5), 1071-1080.

Latorre, R., Muñoz, F., González, C., & Cosmelli, D. (2003). Structure and function of potassium channels in plants: some inferences about the molecular origin of inward rectification in KAT1 channels (Review). Molecular membrane biology, 20(1), 19-25.

Leyman, B., Geelen, D., Quintero, F. J., & Blatt, M. R. (1999). A tobacco syntaxin with a role in hormonal control of guard cell ion channels. Science, 283(5401), 537-540.

Long, S.B., Campbell, E.B., and Mackinnon, R. (2005). Crystal structure of a mammalian voltage-dependent Shaker family K+ channel. Science 309, 897-903.

Munro, S. (1991). Sequences within and adjacent to the transmembrane segment of alpha-2, 6-sialyltransferase specify Golgi retention. The EMBO Journal, 10(12), 3577.

Munro, S., & Pelham, H. R. (1987). A C-terminal signal prevents secretion of luminal ER proteins. Cell, 48(5), 899-907.

Nakamura, R. L., McKendree Jr, W. L., Hirsch, R. E., Sedbrook, J. C., Gaber, R. F., & Sussman, M. R. (1995). Expression of an Arabidopsis potassium channel gene in guard cells. Plant Physiology, 109(2), 371-374.

Palmer, E., & Freeman, T. (2004). Investigation into the use of C-and N-terminal GFP fusion proteins for subcellular localization studies using reverse transfection microarrays. Comparative and functional genomics, 5(4), 342-353.

Petrie, J. R., Shrestha, P., Liu, Q., Mansour, M. P., Wood, C. C., Zhou, X.-R., … Singh, S. P. (2010). Rapid expression of transgenes driven by seed-specific constructs in leaf tissue: DHA production. Plant Methods, 6, 8.

Pilot, G., Pratelli, R., Gaymard, F., Meyer, Y., and Sentenac, H. (2003). Five-group distribution of the Shaker-like K+ channel family in higher plants. J Mol Evol 56, 418-434.

Remy, I., Montmarquette, A., & Michnick, S. W. (2004). PKB/Akt modulates TGF-β signalling through a direct interaction with Smad3. Nature cell biology, 6(4), 358-365.

Roberts, C. S., Rajagopal, S., Smith, L. A., Nguyen, T. A., Yang, W., Nugroho, S., ... & Harcourt, R. L. (1998). A comprehensive set of modular vectors for advanced manipulations and efficient transformation of plants by both Agrobacterium and direct DNA uptake methods. CAMBIA Vector Release Manual Version, 3.

Roelfsema, M. R. G., & Hedrich, R. (2005). In the light of stomatal opening: new insights into 'the Watergate'. New Phytologist, 167(3), 665-691.

Ronzier, E., Corratgé-Faillie, C., Sanchez, F., Prado, K., Brière, C., Leonhardt, N., Thibaud, J.B., and Xiong, T.C. (2014). CPK13, a noncanonical Ca2+-dependent protein kinase, specifically inhibits KAT2 and KAT1 shaker K+ channels and reduces stomatal opening. Plant Physiol 166, 314-326.

Sarrion-Perdigones, A., Falconi, E. E., Zandalinas, S. I., Juárez, P., Fernández-del-Carmen, A., Granell, A., & Orzaez, D. (2011). GoldenBraid: an iterative cloning system for standardized assembly of reusable genetic modules. PloS one, 6(7), e21622.

Sarrion-Perdigones, A., Vazquez-Vilar, M., Palací, J., Castelijns, B., Forment, J., Ziarsolo, P., ... & Orzaez, D. (2013). GoldenBraid 2.0: a comprehensive DNA assembly framework for plant synthetic biology. Plant physiology, 162(3), 1618-1631.

Sato, A., Gambale, F., Dreyer, I. and Uozumi, N. (2010), Modulation of the Arabidopsis KAT1 channel by an activator of protein kinase C in Xenopus laevis oocytes. FEBS Journal, 277: 2318–2328.

Sato, A., Sato, Y., Fukao, Y., Fujiwara, M., Umezawa, T., Shinozaki, K., ... & Uozumi, N. (2009). Threonine at position 306 of the KAT1 potassium channel is essential for channel activity and is a target site for ABA-activated SnRK2/OST1/SnRK2. 6 protein kinase. Biochemical Journal, 424(3), 439-448.

Sato, Y., Sakaguchi, M., Goshima, S., Nakamura, T., & Uozumi, N. (2002). Integration of Shaker-type K+ channel, KAT1, into the endoplasmic reticulum membrane: Synergistic insertion of voltage-sensing segments, S3–S4, and independent insertion of pore-forming segments, S5–P–S6. Proceedings of the National Academy of Sciences, 99(1), 60-65.

Schroeder, J.I., Allen, G.J., Hugouvieux, V., Kwak, J.M., and Waner, D. (2001). Guard Cell Signaling Transduction. Annu Rev Plant Physiol Plant Mol Biol 52, 627-658.

Sharma, T., Dreyer, I., & Riedelsberger, J. (2013). The role of K(+) channels in uptake and redistribution of potassium in the model plant Arabidopsis thaliana. Frontiers in Plant Science, 4(June), 224.

Sottocornola, B., Gazzarrini, S., Olivari, C., Romani, G., Valbuzzi, P., Thiel, G., & Moroni, A. (2008). 14-3-3 proteins regulate the potassium channel KAT1 by dual modes. Plant Biology, 10(2), 231-236.

Sutter, J. U., Campanoni, P., Tyrrell, M., & Blatt, M. R. (2006). Selective mobility and sensitivity to SNAREs is exhibited by the Arabidopsis KAT1 K+ channel at the plasma membrane. The Plant Cell, 18(4), 935-954.

Sutter, J. U., Sieben, C., Hartel, A., Eisenach, C., Thiel, G., & Blatt, M. R. (2007). Abscisic acid triggers the endocytosis of the Arabidopsis KAT1 K+ channel and its recycling to the plasma membrane. Current Biology, 17(16), 1396-1402.

Uozumi, N., Nakamura, T., Schroeder, J. I., & Muto, S. (1998). Determination of transmembrane topology of an inward-rectifying potassium channel from Arabidopsis thaliana based on functional expression in Escherichia coli. Proceedings of the National Academy of Sciences, 95(17), 9773-9778.

Véry, A. A., Nieves-Cordones, M., Daly, M., Khan, I., Fizames, C., & Sentenac, H. (2014). Molecular biology of K+ transport across the plant cell membrane: What do we learn from comparison between plant species? Journal of Plant Physiology, 171(9), 748–769.

Véry, A.A., and Sentenac, H. (2003). Molecular mechanisms and regulation of K+ transport in higher plants. Annu Rev Plant Biol 54, 575-603.

Wang, Y., Hills, A., and Blatt, M.R. (2014). Systems analysis of guard cell membrane transport for enhanced stomatal dynamics and water use efficiency. Plant Physiol *164*, 1593-1599.

Wiemann, S., Bechtel, S., Bannasch, D., Pepperkok, R., & Poustka, A. (2003). The German cDNA network: cDNAs, functional genomics and proteomics. Journal of structural and functional genomics, 4(2-3), 87-96.

Yarmola, E. G., Somasundaram, T., Boring, T. A., Spector, I., & Bubb, M. R. (2000). Actin-latrunculin A structure and function differential modulation of actin-binding protein function by latrunculin A. Journal of Biological Chemistry, 275(36), 28120-28127.

Zhang, B., Karnik, R., Wang, Y., Wallmeroth, N., Blatt, M. R., & Grefen, C. (2015). The Arabidopsis R-SNARE VAMP721 interacts with KAT1 and KC1 K+ channels to moderate K+ current at the plasma membrane. The Plant Cell, 27(6), 1697-1717.

Zhang, X., Ma, J., & Berkowitz, G. A. (1999). Evaluation of Functional Interaction between K+ Channel α-and β-Subunits and Putative Inactivation Gating by Co-Expression in Xenopus laevisOocytes. Plant physiology, 121(3), 995-1002.

8. Annex

8.1. Sequencing primer

In order to sequence the KAT1 GB parts pUPD2+KAT1 B3B4 and pUPD2+KAT1 B3B4B5, the following primer that anneals from the nucleotide 1831 of the KAT1 sequence was used.

KAT1-1831-F *: 5'-AAGAGAGTTACCATCCAC -3' Tm = 51°C

8.2. GoldenBraid Vectors

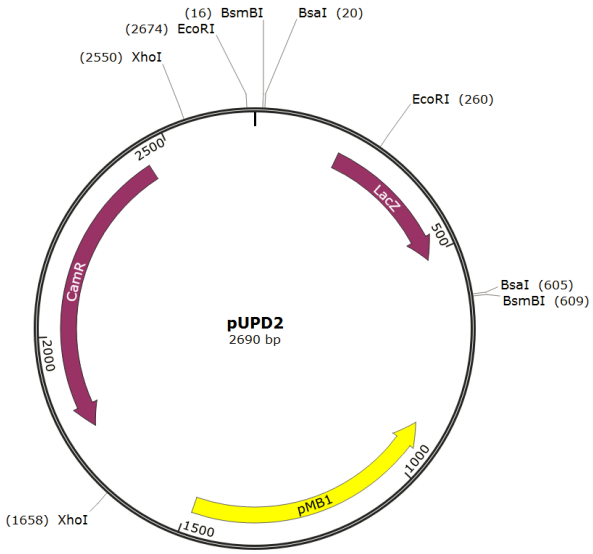

Figure 8.1. pUPD2 plasmid map. *Restriction sites for BsaI and BsmBI, and for EcoRI and XhoI that were used in the digestion analysis.*

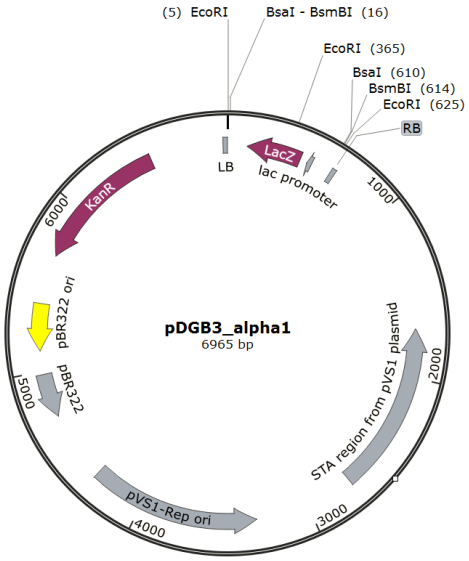

Figure 8.2. pDGB3_alpha1 plasmid map. *Restriction sites for BsmBI and BsaI, and for EcoRI that was used in the digestion analysis.*